of apoptosis [8], induction of angiogenesis [9] and attenuation of myocardial hypertrophy [10]. Interestingly, AM has also been shown to decrease endothelial hyperpermeability in the heart [11]. These findings raise the possibility that infusion of AM may attenuate myocardial inflammation and edema in acute myocarditis. Although previous findings have demonstrated that infusion of AM is effective for heart failure, its therapeutic effects in acute myocarditis are still unknown.

Experimental autoimmune myocarditis can be induced in rats by immunizing them with cardiac myosin, providing a model that resembles human giant cell myocarditis [12,13]. Although the majority of acute myocarditis is linked to a viral infection such as coxsackievirus B3, this viral infection can in some cases cause an autoimmune myocarditis with chronic myocardial inflammation without viral persistence, due to the exposure of autoantigens such as cardiac myosin to the immune system [14,15].

Thus, the purposes of this study were 1) to investigate whether infusion of AM improves cardiac function and pathological findings including myocardial inflammation and edema in rats with myosin-induced myocarditis, and 2) to investigate the underlying mechanisms responsible for the effects of AM.

2. Methods

2.1. Experimental autoimmune myocarditis

Purified cardiac myosin from the ventricular muscle of pig hearts was prepared according to a procedure described previously [16]. The antigen was dissolved at a concentration of 20 mg/ml in phosphate-buffered saline (PBS) containing 0.3 M KCl mixed with an equal volume of complete Freund's adjuvant (CFA) containing 11 mg/ml of *Mycobacterium tuberculosis* (Difco Laboratories, Sparks, MD, USA).

Male 10-week-old Lewis rats were used in the present study. Rats were anesthetized by intraperitoneal injection of pentobarbital (30 mg/kg) and were given an injection of either 0.2 ml of antigen–adjuvant emulsion or saline mixed with CFA into the footpad. One week after myosin injection, an osmotic pump (Alzet, Cupertino, CA, USA) was filled with either AM (0.05 μg/kg/min) or PBS for 2 weeks, and implanted subcutaneously between the scapulae. This protocol resulted in the creation of 3 groups ($n=11$ in each group): sham rats given PBS (sham group), myosin-treated rats given PBS (control group), and myosin-treated rats given AM (AM group). The dose of AM used in this study has anti-apoptotic effects without significant hypotension [8]. The investigation conforms with the Guide for the Care and Use of Laboratory Animals published by the US National Institutes of Health.

2.2. Histopathology

After completion of hemodynamic measurements on day 21 post-myosin injection, the heart was excised above the origin of the great vessels, and ventricular weight was recorded. Midventricular portions of the heart were formalin-fixed and embedded in paraffin, and 4 μm-sections were cut and stained with hematoxylin and eosin (H&E). H&E-stained sections were graded by a cardiovascular pathologist (H.I-U.) as described previously [17]. Briefly, coagulation necrosis, granulation, inflammation and edema were evaluated without knowledge of the experimental groups on the following scale: 0, no or questionable presence; 1, limited focal distribution less than 25% area of the section; 2, intermediate severity covering less than 50% area of the section; 3, intermediate severity covering greater than 50% and less than 75% area of the section; and 4, coalescent and extensive foci more than 75% area to the entirety of the transversely sectioned ventricular tissue (5 fields per rat, $n=8$ in each group).

2.3. Picrosirius red staining

Paraffin-embedded sections were submitted for picrosirius staining for total collagen distribution. Slides were hydrated, placed in Weigert's iron hematoxylin and in Bouin's fluid (70% saturated aqueous picric acid, 5% acetic acid, 25% formalin) for 10 min. The slides were rinsed in distilled water and placed in 0.025% picrosirius red solution overnight. The sections were rinsed, dehydrated, cleared, and mounted. Amount of collagen stain was quantitated using image analysis software on high-powered (×200) cross-sectional images (10 fields per rat, $n=5$ in each group).

2.4. Immunohistochemistry

Paraffin-embedded heart sections were washed in increasing concentrations of ethanol and then in PBS. Immunohistochemical staining of the sections was performed with antibodies raised against macrophage chemoattractant protein-1 (MCP-1) (BD Bioscience Pharmingen, San Jose, CA, USA) or CD68 (DakoCytomation, Glostrup, Denmark), a marker of monocytes and macrophages. The number of CD68-positive cells was counted with a light microscope (×200, 10 fields per rat, $n=6$ in each group). To detect capillary endothelial cells, immunohistochemical staining of the sections was performed with a rabbit polyclonal antibody raised against von Willebrand factor (vWF, DakoCytomation). The number of capillary vessels was counted using a light microscope (×200, 10 fields per rat, $n=6$ in each group).

2.5. Western blot analysis

Western blot was performed as previously described [18]. Briefly, LV tissues were homogenized in 0.1% Tween-20 with a protease inhibitor, loaded (40 μg) on a 7.5% sodium dodecyl sulfate-polyacrylamide gel, and blotted onto a polyvinylidene fluoride membrane (Millipore, Billerica, MA, USA). After blocking for 2 h, membranes were incubated with MMP-2 (Laboratory Vision, Fremont, CA, USA) or MMP-9

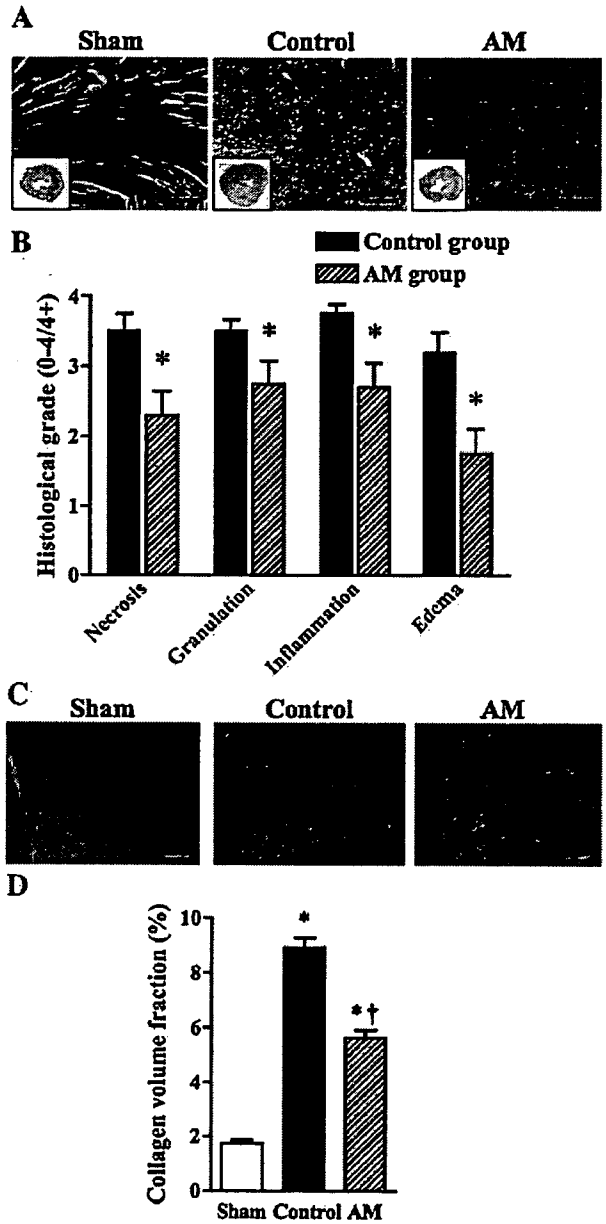

Fig. 1. Pathological findings in acute myocarditis after AM infusion. A: Representative H&E staining of myocardial sections showed markedly decreased inflammation and tissue necrosis in AM-treated hearts as compared to control hearts. Insets are transverse sections of myocardial freewall. B: Semi-quantitative histological grades for necrosis and tissue granulation as well as for inflammation and edema were significantly lower in AM-treated hearts as compared to control hearts ($n=8$ in each group). Sham tissues exhibited no measurable pathological changes. Data are mean±S.E. *, $P<0.05$ *vs.* control. C: Representative picrosirius staining showed decreased collagen deposition in AM-treated hearts as compared to control hearts. D: Collagen volume fraction in 10 random representative fields (×200) confirmed a significant decrease in AM-treated hearts *vs.* control hearts ($n=5$ in each group). Scale bars: 50 μm. Data are mean±S.E. *, $P<0.05$ *vs.* sham; †, $P<0.05$ *vs.* control.

(Chemicon, Temecula, CA, USA) rabbit polyclonal antibodies (1:200), then incubated with peroxidase labeled with secondary antibody (1:1000). Positive protein bands were visualized with an ECL kit (GE Healthcare, Piscataway, NJ, USA) and measured by densitometry. A mouse polyclonal antibody against β-actin (Santa Cruz Biotechnology, Santa Cruz, CA, USA) was used as a control ($n=5$ in each group).

2.6. Quantitative real-time reverse transcription-polymerase chain reaction (RT-PCR)

Heart tissues ($n=5$ in each group) were homogenized with TissueLyser (Qiagen, Hilden, Germany). Total RNA was extracted using RNeasy Mini Kit (Qiagen), followed by reverse transcription into cDNA using the avian myeloblastosis virus transcriptase (Ambion, Austin, TX, USA), according to the manufacturers' protocol. PCR amplification was performed in 50 μl containing 1 μl of cDNA and 25 μl of Power SYBR Green PCR Master Mix (Applied Biosystems, Foster City, CA, USA). The following sequence-specific primers were used for TGF-β, as described previously [19]: forward, 5′-GTTCTTCAATACGTCAGACATTCG-3′; reverse, 5′-CATTATCTTTGCTGTCACAAGAGC-3′. Glyceraldehyde 3-phosphate dehydrogenase (GAPDH) mRNA amplified from the same samples was served as an internal control: forward, 5′-GAACATCATCCCTGCATCCA-3′; reverse, 5′-CCAGTGAGCTTCCCGTTCA-3′. After an initial denaturation at 95 °C for 10 min, a 2-step cycle procedure was used (denaturation at 95 °C for 15 s, annealing and extension at 60 °C for 1 min) for 40 cycles in a 7700 sequence detector (Applied Biosystems). The data were analyzed with Sequence Detection Systems software.

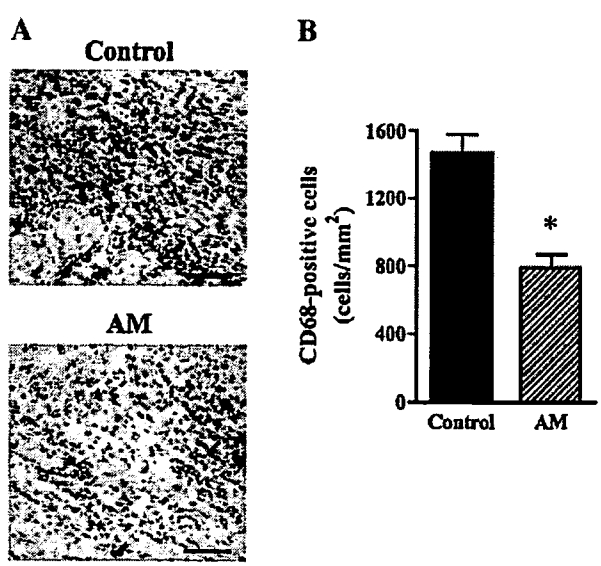

Fig. 2. Infiltration of inflammatory cells in myocardium. A: Immunohistochemical analysis of CD68-positive cell infiltration in myocardium. AM infusion markedly attenuated the increase in CD68-positive cells in myocarditic hearts. Scale bars: 50 μm. B: Semi-quantitative analysis of CD68-positive cell infiltration. CD68-positive cells in 10 random representative high-power fields (×200) confirmed a significant decrease in AM-treated hearts *vs.* control hearts ($n=6$ in each group). Data are mean±S.E. *, $P<0.05$ *vs.* control.

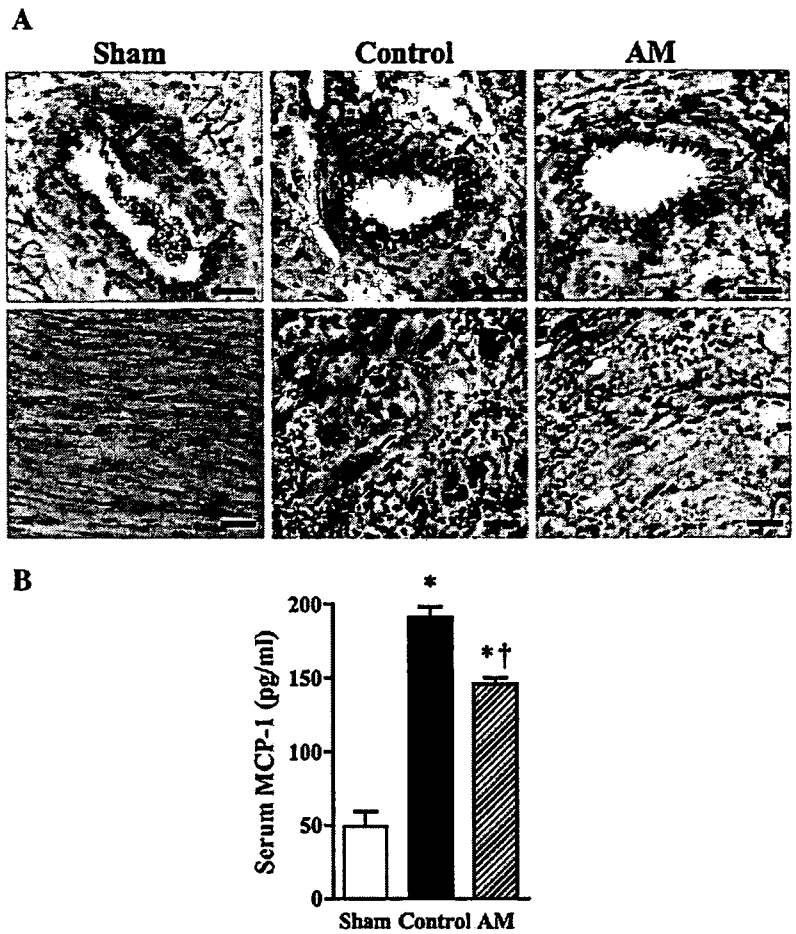

Fig. 3. Effects of AM infusion on MCP-1 expression. A: Representative myocardial sections immunohistochemically stained with anti-MCP-1 antibody showed increased vascular endothelial and myocyte staining of MCP-1 (arrows) and the presence of giant cells (arrowheads) in control hearts as compared to AM-treated hearts. Sham hearts showed subtle endothelial staining. Scale bars: 20 μm. B: Serum MCP-1 level was greatly increased in myocarditic rats. However, the increase in serum MCP-1 was significantly attenuated by AM infusion ($n=6$ in each group). Data are mean±S.E. *, $P<0.05$ *vs.* sham; †, $P<0.05$ *vs.* control.

2.7. Enzyme-linked immunosorbent assay (ELISA)

To investigate the effect of AM infusion on serum MCP-1 level, blood was drawn from the heart before excision ($n=6$ in each group). Blood was centrifuged and serum samples were frozen and stored at −80 °C. Serum MCP-1 level was measured by ELISA according to the manufacturer's instructions (Invitrogen, Carlsbad, CA, USA).

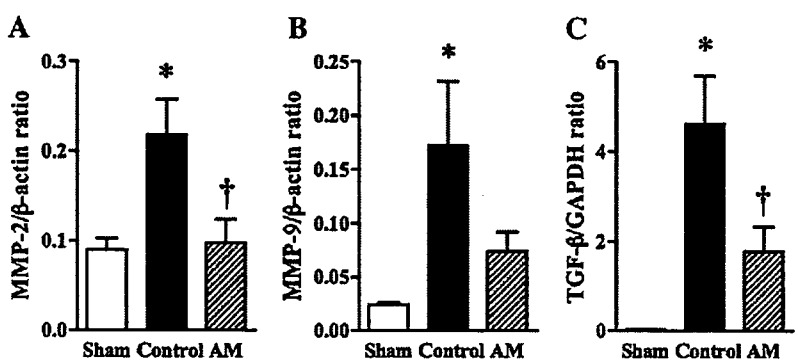

Fig. 4. Effects of AM infusion on MMP and TGF-β expression. A and B: Western blot analysis for MMP-2 (A) and -9 (B) expression. Levels of MMP-2 and -9 were significantly increased in control hearts. MMP-2 expression was markedly decreased by AM infusion, and MMP-9 expression tended to be decreased after AM infusion ($n=5$ in each group). C: Quantitative real-time reverse transcription-polymerase chain reaction (RT-PCR) for TGF-β expression. Expression of TGF-β was increased in myocarditis and significantly decreased by AM treatment ($n=5$ in each group). Data are mean±S.E. *, $P<0.05$ *vs.* sham; †, $P<0.05$ *vs.* control.

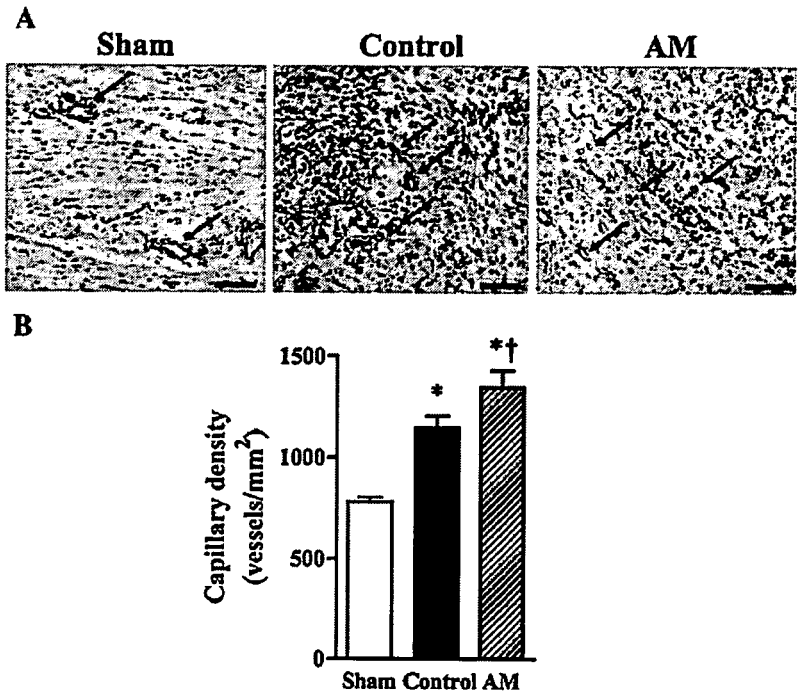

Fig. 5. Increased endothelial regeneration with AM infusion. A: Immunohistochemical demonstration of von Willebrand factor in myocardium. Arrows indicate microvasculature. Scale bars: 20 μm. B: Capillary density measured in 10 random representative high-power fields (×200) showed a significant increase in control hearts and a further increase in AM-treated hearts *vs.* sham hearts (n=6 in each group). Data are mean±S.E. *, P<0.05 *vs.* sham; †, P<0.05 *vs.* control.

2.8. Hemodynamic study

Hemodynamic measurements were taken on day 21 post-myosin injection (n=7 in each group). Rats were anesthetized by intraperitoneal injection of pentobarbital sodium (30 mg/kg) as a supplement to maintain mild anesthesia. A 1.5 Fr micromanometer-tipped catheter (Millar Instruments, Houston, TX, USA) was advanced into the left ventricle through the right carotid artery, and a polyethylene catheter (PE-50) was advanced into the right ventricle through the right jugular vein to measure right ventricular pressure. Heart rate was also monitored by electrocardiography. As hemodynamic indices, heart rate, mean arterial pressure, LV end-diastolic pressure, maximum dP/dt, and minimum dP/dt were used.

2.9. Echocardiography

Echocardiography was performed on day 21 post-myosin injection. A 12-MHz probe was placed in the left 4th intercostal space for M-mode imaging using 2D echocardiography (Sonos 5500, Philips, Bothell, WA, USA). M-mode tracings were obtained at the level of the papillary muscles. Anterior and posterior end-diastolic wall thickness, left ventricular (LV) end-diastolic and end-systolic dimension, LV fractional shortening (FS), and LV ejection fraction (EF) were measured in three consecutive cardiac cycles by the American Society for Echocardiology leading-edge method (n=10 in each group). EF and FS were calculated from the following formula, respectively:

$$EF = (\text{end-diastolic volume} - \text{end-systolic volume}) / \text{end-diastolic volume}$$

$$FS = (\text{end-diastolic diameter} - \text{end-systolic diameter}) / \text{end-diastolic diameter}$$

2.10. Statistical analysis

All data were expressed as mean±S.E. Comparisons of parameters among the groups were made by one-way

Table 1
Physiological profiles of three experimental groups

	Sham	Control	AM
Body weight, g	236±2	197±2*	199±2*
Ventricular weight, g	0.70±0.01	1.28±0.02*	1.15±0.03*†
Lung/body weight	4.9±0.4	4.9±0.5	5.0±0.8
Heart rate, bpm	432±10	373±11	393±6
MAP, mm Hg	103±3	77±5*	93±3†
LVSP, mm Hg	127±3	103±5*	117±3†
LVEDP, mm Hg	4±1	21±5*	14±3

Sham, sham rats given vehicle; Control, myosin-treated rats given vehicle; AM, myosin-treated rats given AM; MAP, mean arterial pressure; LVSP, left ventricular systolic pressure; LVEDP, left ventricular end-diastolic pressure. Data are mean±S.E. *P<0.05 *vs.* sham; †P<0.05 *vs.* control. n=7 in each group.

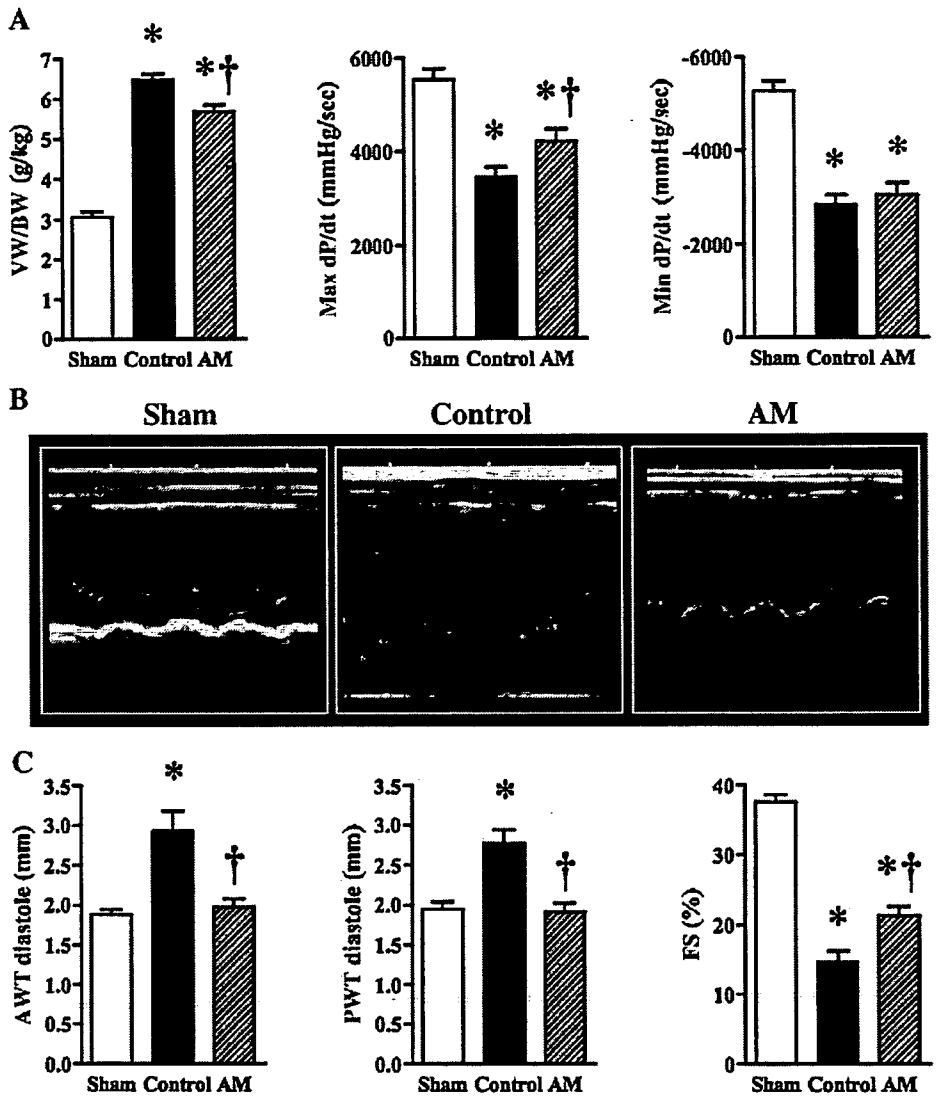

Fig. 6. Effects of AM infusion on physiologic properties and hemodynamic parameters. A: Effects of AM infusion on physiologic properties ($n=7$ in each group). B: Representative echocardiographic images show wall thickening and poor movement in myocarditis and improvement with AM treatment. C: Effects of AM infusion on echocardiographic findings ($n=10$ in each group). VW/BW, ventricular weight/body weight ratio; Max dP/dt, maximum dP/dt; Min dP/dt, minimum dP/dt; AWT, anterior wall thickness; PWT, posterior wall thickness; %FS, %fractional shortening. Data are mean ± S.E. *, $P<0.05$ *vs.* sham; †, $P<0.05$ *vs.* control.

ANOVA, followed by Newman–Keuls' test. Comparisons of parameters between two groups were made by Student's *t*-test. A value of $P<0.05$ was considered statistically significant.

3. Results

3.1. Histopathological improvement after AM infusion

Sections of left ventricular tissue demonstrated substantial myocardial necrosis, infiltration of inflammatory cells and edema in the control group, which was significantly limited primarily to areas directly adjacent to arterial vessels with AM treatment (Fig. 1, panel A). Blinded histological grading confirmed decreased myocyte necrosis, granulation, inflammation and tissue edema in the AM group as compared in the control group (Fig. 1, panel B). Picrosirius red staining revealed increased collagen deposition in the control group (Fig. 1, panel C). However, AM infusion attenuated collagen deposition in the myocardium (Fig. 1, panel D).

Table 2
Echocardiographic findings

	Sham	Control	AM
LVDd, mm	4.9±0.1	6.5±0.2*	7.3±0.3*†
LVDs, mm	3.1±0.1	5.7±0.2*	5.7±0.3*†
EF, %	75±1	35±3*	52±2*†

Sham, sham rats given vehicle; Control, myosin-treated rats given vehicle; AM, myosin-treated rats given AM; LVDd, left ventricular diastolic dimension; LVDs, left ventricular systolic dimension; EF, ejection fraction. Data are mean ± S.E. *$P<0.05$ *vs.* sham; †$P<0.05$ *vs.* control. $n=10$ in each group.

3.2. Infiltration of CD68-positive cells in myocardium

A significant decrease in infiltration of CD68-positive inflammatory cells was observed in the AM group as compared to the control group (790±80 *vs.* 1468±109 cells/mm^2; Fig. 2, panel A and B). Sham tissues showed little or no myocardial CD68 positivity (data not shown).

3.3. Expression of MCP-1 after AM infusion

The expression of MCP-1 was increased in myocarditis; it was localized to the vascular endothelium and also in myocytes surrounding and adjacent to the areas of inflammation (Fig. 3, panel A). Heart sections in the AM group showed a partial decrease in MCP-1 expression. Serum MCP-1 level was greatly increased in the control group, whereas a significant decrease was observed in the AM group (Fig. 3, panel B).

3.4. Effects of AM infusion on MMPs and TGF-β expression

Western blotting analysis revealed that myocardial levels of MMP-2 and -9 were significantly increased in the control group. MMP-2 expression was markedly decreased by AM infusion, and MMP-9 expression tended to be decreased after AM infusion (Fig. 4, panel A). Quantitative real-time RT-PCR analysis demonstrated increased expression of TGF-β in the heart of the control group which was significantly attenuated by AM treatment (Fig. 4, panel B). AM infusion did not significantly influence cardiac expression of IL-1β and TNF-α (data not shown).

3.5. Angiogenesis induced by AM infusion

To determine the effect of AM treatment on angiogenesis, vWF-stained heart sections were subjected to capillary density counting. Capillary density was increased in the control group, particularly in areas directly adjacent to tissue necrosis (1146±57 *vs.* 782±21 cells/mm^2, Fig. 5, panel A and B). However, in AM-treated tissues, capillary density was further significantly increased not only in the peri-necrotic areas but also in apparently healthy myocardium (1347±82 *vs.* 1146±57cells/mm^2), suggesting that stimulation of angiogenesis was further augmented by AM treatment.

3.6. Heart weight and hemodynamics after AM infusion

The physiological and catheter-derived functional properties on day 21 post-myosin injection are summarized in Table 1 and Fig. 6, panel A. Myocarditic hearts showed significantly increased heart weight to body weight ratio, which was decreased by AM treatment. AM treatment also significantly improved maximum d*P*/d*t*. For both minimum d*P*/d*t* and LVEDP, we did not find significant differences. On echocardiography, AM administration significantly attenuated increased wall thickness after acute myocarditis. AM significantly improved LV fractional shortening and ejection fraction, although LVDd did not significantly differ between control and AM groups (Table 2 and Fig. 6, panel B and C).

4. Discussion

In the present study, AM treatment showed the following effects in acute myocarditis: 1) reduced necrosis, inflammation and edema in the myocardium; 2) attenuated expression of MCP-1, MMP-2 and TGF-β; 3) increased capillary density suggestive of angiogenesis; and 4) improved cardiac function.

This experimental autoimmune myocarditis model is triphasic, consisting of an antigen priming phase from days 0 to 14, an autoimmune response phase from days 14 to 21, and a reparative phase thereafter, associated chronically with a dilated cardiomyopathy phenotype [20]. MCP-1 expression is increased in the heart from days 15 to 27 post-myosin injection, and serum MCP-1 level is elevated from days 15 to 24 [21]. We treated rats with AM at 1 week after myosin injection, corresponding to an early time point in the disease process. Pathological examination demonstrated that infusion of AM attenuated myocyte necrosis and inflammation in acute myocarditis. This observation was supported by a decrease in infiltration of CD68-positive inflammatory cells in the myocardium. Interestingly, both MCP-1 expressions in the myocardium and serum MCP-1 level were decreased after AM infusion. MCP-1 is a member of the C–C subfamily of chemokines with chemoattractant activity for major inflammatory cells such as monocytes and T lymphocytes [22], and this model of acute myocarditis has previously been shown to be associated with MCP-1 [21]. Thus, the decrease in CD68-positive cell infiltration in the myocardium following this treatment may be attributable to inhibition of MCP-1 production by AM. The inhibitory effect of AM on MCP-1 expression is consistent with a previous *in vitro* study showing that AM inhibited pressure-induced MCP-1 expression in mesangial cells [23]. Recently, it has been demonstrated that AM has anti-inflammatory effects through modulation of macrophage migration inhibitory factor secretion [24]. Importantly, overexpression of MCP-1 induces myocarditis and subsequent development of heart failure [25]. These findings suggest that the inhibitory effect on MCP-1 expression and subsequent anti-inflammatory effect of AM are possible mechanisms of the improvement in acute myocarditis.

We found a significant increase in heart weight to body weight ratio and wall thickness 3 weeks after myosin injection. These results indicate exaggerated edematous changes in myocarditic hearts. Infusion of AM reduced overall heart weight to body weight ratio and wall thickness in myocarditic hearts and attenuated histological edematous changes. Earlier studies have demonstrated that AM decreases vascular congestion and endothelial hyperpermeability in the heart [11], reduces hyperpermeability of cultured endothelial cells and inhibits pulmonary edema [26]. Thus, it is interesting to speculate that the attenuation of edematous changes in the

heart may be attributable to reduction of endothelial hyperpermeability by AM.

In the present study, AM infusion significantly increased the capillary density in myocarditic hearts. In fact, earlier studies have demonstrated angiogenic properties of AM *in vitro* and *in vivo* [27–29]. Importantly, improvement in myocardial vascular supply has been shown to decrease necrosis and inflammation in viral myocarditis [30,31]. These results suggest that AM-induced angiogenesis in the myocardium may be responsible for the improvement in acute myocarditis, which was indicated by reduced necrosis and inflammation in myocarditic hearts.

As previously mentioned, experimental autoimmune myocarditis chronically develops into a dilated cardiomyopathy phenotype [20]. MMPs have been associated with left ventricular remodeling [32] and here we showed increased expression of MMP-2 and -9 as well as increased collagen deposition in myocarditic hearts. In the present study, AM treatment significantly reduced both MMP-2 expression and collagen deposition. In addition, our observation demonstrated that the expression of TGF-β, a profibrogenic factor, was also attenuated by AM treatment. It has been demonstrated that AM decreases the expression of TGF-β in experimental mesangioproliferative glomerulonephritis [33]. These results suggest that AM may have beneficial effects on myocardium, possibly through regulation of factors involved in LV remodeling. In the present study, LVDd did not significantly differ between the control and AM groups. However, it should be noted that AM significantly reduced wall thickness possibly due to reduction of myocardial edema, leading to a slight increase in the inner diameter of the LV and a significant increase in ejection fraction. The major effect of AM was to reduce myocardial edema but not remodeling, despite reducing biochemical markers of remodeling.

Earlier studies have shown that short-term infusion of AM decreases arterial pressure and increases cardiac output in patients with acute heart failure [5]. These findings suggest that the improvement in cardiac function after acute myocarditis may be mediated partly by the hemodynamic effects of AM. However, despite the well-characterized vasorelaxant properties of AM [4], there was a significant increase in mean arterial pressure after AM treatment in our model. These findings suggest that AM induced limited direct hemodynamic action. Taking these findings together, the improvement of cardiac function after AM treatment may have been mediated by the improvement of pathological findings including necrosis, inflammation and edema in the myocardium rather than by AM-induced hemodynamic effects.

In conclusion, infusion of AM improved cardiac function and pathological findings including inflammatory infiltration and edema in a rat model of acute myocarditis. The beneficial effects of AM may occur at least in part by inhibitory effects on MCP-1, MMP-2 and TGF-β, and by enhancement of angiogenesis after acute myocarditis. Thus, infusion of AM may be a potent therapeutic strategy for acute myocarditis.

Acknowledgements

This work was supported by research grants for Cardiovascular Disease (16C-6 and 17A-1) and Comprehensive Research on Aging and Health from the Ministry of Health, Labour and Welfare, the Program for Promotion of Fundamental Studies in Health Sciences of the National Institute of Biomedical Innovation (NIBIO); and Health and Labor Sciences Research Grants (Human Genome Tissue Engineering 009).

References

[1] Levi D, Alejos J. Diagnosis and treatment of pediatric viral myocarditis. Curr Opin Cardiol 2001;16:77–83.
[2] Liu Z, Yuan J, Yanagawa B, Qiu D, McManus BM, Yang D. Coxsackievirus-induced myocarditis: new trends in treatment. Expert Rev Anti Infect Ther 2005;3:641–50.
[3] Feldman AM, McNamara D. Myocarditis. N Engl J Med 2000;343: 1388–98.
[4] Kitamura K, Kangawa K, Kawamoto M, Ichiki Y, Nakamura S, Matsuo H, et al. Adrenomedullin: a novel hypotensive peptide isolated from human pheochromocytoma. Biochem Biophys Res Commun 1993;192:553–60.
[5] Nagaya N, Satoh T, Nishikimi T, Uematsu M, Furuichi S, Sakamaki F, et al. Hemodynamic renal and hormonal effects of adrenomedullin infusion in patients with congestive heart failure. Circulation 2000;101:498–503.
[6] Oya H, Nagaya N, Furuichi S, Nishikimi T, Ueno K, Nakanishi N, et al. Comparison of intravenous adrenomedullin with atrial natriuretic peptide in patients with congestive heart failure. Am J Cardiol 2000;86:94–8.
[7] Clementi G, Caruso A, Cutuli VM, Prato A, Mangano NG, Amico-Roxas M. Antiinflammatory activity of adrenomedullin in the acetic acid peritonitis in rats. Life Sci 1999;65:PL203–8.
[8] Okumura H, Nagaya N, Itoh T, Okano I, Hino J, Mori K, et al. Adrenomedullin infusion attenuates myocardial ischemia/reperfusion injury through the phosphatidylinositol 3-kinase/Akt-dependent pathway. Circulation 2004;109:242–8.
[9] Iwase T, Nagaya N, Fujii T, Itoh T, Ishibashi-Ueda H, Yamagishi M, et al. Adrenomedullin enhances angiogenic potency of bone marrow transplantation in a rat model of hindlimb ischemia. Circulation 2005;111: 356–62.
[10] Tsuruda T, Kato J, Kitamura K, Kuwasako K, Imamura T, Koiwaya Y, et al. Adrenomedullin: a possible autocrine or paracrine inhibitor of hypertrophy of cardiomyocytes. Hypertension 1998;31:505–10.
[11] Chu DQ, Smith DM, Brain SD. Studies of the microvascular effects of adrenomedullin and related peptides. Peptides 2001;22:1881–6.
[12] Kodama M, Matsumoto Y, Fujiwara M, Zhang SS, Hanawa H, Itoh E, et al. Characteristics of giant cells and factors related to the formation of giant cells in myocarditis. Circ Res 1991;69:1042–50.
[13] Kodama M, Matsumoto Y, Fujiwara M, Masani F, Izumi T, Shibata A. A novel experimental model of giant cell myocarditis induced in rats by immunization with cardiac myosin fraction. Clin Immunol Immunopathol 1990;57:250–62.
[14] Fairweather D, Kaya Z, Shellam GR, Lawson CM, Rose NR. From infection to autoimmunity. J Autoimmun 2001;16:175–86.
[15] Cunningham MW. T cell mimicry in inflammatory heart disease. Mol Immunol 2004;40:1121–7.
[16] O'Connell JBRD. Myocarditis and specific myocardial diseases. New York: McGraw-Hill; 1994. Pages.
[17] Yanagawa B, Spiller OB, Choy J, Luo H, Cheung P, Zhang HM, et al. Coxsackievirus B3-associated myocardial pathology and viral load reduced by recombinant soluble human decay-accelerating factor in mice. Lab Invest 2003;83:75–85.
[18] Nagaya N, Kangawa K, Itoh T, Iwase T, Murakami S, Miyahara Y, et al. Transplantation of mesenchymal stem cells improves cardiac function in a rat model of dilated cardiomyopathy. Circulation 2005;112:1128–35.

[19] Hanawa H, Abe S, Hayashi M, Yoshida T, Yoshida K, Shiono T, et al. Time course of gene expression in rat experimental autoimmune myocarditis. Clin Sci (Lond) 2002;103:623–32.
[20] Kodama M, Hanawa H, Saeki M, Hosono H, Inomata T, Suzuki K, et al. Rat dilated cardiomyopathy after autoimmune giant cell myocarditis. Circ Res 1994;75:278–84.
[21] Fuse K, Kodama M, Hanawa H, Okura Y, Ito M, Shiono T, et al. Enhanced expression and production of monocyte chemoattractant protein-1 in myocarditis. Clin Exp Immunol 2001;124:346–52.
[22] Rollins BJ. Chemokines. Blood 1997;90:909–28.
[23] Iwamoto M, Osajima A, Tamura M, Suda T, Ota T, Kanegae K, et al. Adrenomedullin inhibits pressure-induced mesangial MCP-1 expression through activation of protein kinase A. J Nephrol 2003;16:673–81.
[24] Wong LY, Cheung BM, Li YY, Tang F. Adrenomedullin is both proinflammatory and antiinflammatory: its effects on gene expression and secretion of cytokines and macrophage migration inhibitory factor in NR8383 macrophage cell line. Endocrinology 2005;146:1321–7.
[25] Kolattukudy PE, Quach T, Bergese S, Breckenridge S, Hensley J, Altschuld R, et al. Myocarditis induced by targeted expression of the MCP-1 gene in murine cardiac muscle. Am J Pathol 1998;152:101–11.
[26] Hippenstiel S, Witzenrath M, Schmeck B, Hocke A, Krisp M, Krull M, et al. Adrenomedullin reduces endothelial hyperpermeability. Circ Res 2002;91:618–25.
[27] Kim W, Moon SO, Sung MJ, Kim SH, Lee S, Kim HJ, et al. Protective effect of adrenomedullin in mannitol-induced apoptosis. Apoptosis 2002;7:527–36.
[28] Tokunaga N, Nagaya N, Shirai M, Tanaka E, Ishibashi-Ueda H, Harada-Shiba M, et al. Adrenomedullin gene transfer induces therapeutic angiogenesis in a rabbit model of chronic hind limb ischemia: benefits of a novel nonviral vector gelatin. Circulation 2004;109:526–31.
[29] Nagaya N, Mori H, Murakami S, Kangawa K, Kitamura S. Adrenomedullin: angiogenesis and gene therapy. Am J Physiol Regul Integr Comp Physiol 2005;288:R1432–7.
[30] Lee JK, Zaidi SH, Liu P, Dawood F, Cheah AY, Wen WH, et al. A serine elastase inhibitor reduces inflammation and fibrosis and preserves cardiac function after experimentally-induced murine myocarditis. Nat Med 1998;4:1383–91.
[31] Ono K, Matsumori A, Shioi T, Furukawa Y, Sasayama S. Contribution of endothelin-1 to myocardial injury in a murine model of myocarditis: acute effects of bosentan an endothelin receptor antagonist. Circulation 1999;100:1823–9.
[32] Tsuruda T, Costello-Boerrigter LC, Burnett JC. Matrix metalloproteinases: pathways of induction by bioactive molecules. Heart Fail Rev 2004;9:53–61.
[33] Plank C, Hartner A, Klanke B, Geissler B, Porst M, Amann K, et al. Adrenomedullin reduces mesangial cell number and glomerular inflammation in experimental mesangioproliferative glomerulonephritis. Kidney Int 2005;68:1086–95.

Am J Physiol Lung Cell Mol Physiol 293: L446–L452, 2007.
First published June 8, 2007; doi:10.1152/ajplung.00412.2005.

Adrenomedullin ameliorates lipopolysaccharide-induced acute lung injury in rats

Takefumi Itoh,[1,2] Hiroaki Obata,[1,3] Shinsuke Murakami,[1,2] Kaoru Hamada,[2] Kenji Kangawa,[4] Hiroshi Kimura,[2] and Noritoshi Nagaya[1,5]

[1]*Department of Regenerative Medicine and Tissue Engineering, National Cardiovascular Center Research Institute, Osaka, Japan;* [2]*Second Department of Internal Medicine, Nara Medical University, Nara, Japan;* [3]*Division of Cardiology, Niigata University Graduate School of Medical and Dental Sciences, Niigata, Japan; and Departments of* [4]*Biochemistry and* [5]*Internal Medicine, National Cardiovascular Center, Osaka, Japan*

Submitted 26 September 2005; accepted in final form 5 June 2007

Itoh T, Obata H, Murakami S, Hamada K, Kangawa K, Kimura H, Nagaya N. Adrenomedullin ameliorates lipopolysaccharide-induced acute lung injury in rats. *Am J Physiol Lung Cell Mol Physiol* 293: L446–L452, 2007. First published June 8, 2007; doi:10.1152/ajplung.00412.2005.—Adrenomedullin (AM), an endogenous peptide, has been shown to have a variety of protective effects on the cardiovascular system. However, the effect of AM on acute lung injury remains unknown. Accordingly, we investigated whether AM infusion ameliorates lipopolysaccharide (LPS)-induced acute lung injury in rats. Rats were randomized to receive continuous intravenous infusion of AM (0.1 $\mu g \cdot kg^{-1} \cdot min^{-1}$) or vehicle through a microosmotic pump. The animals were intratracheally injected with either LPS (1 mg/kg) or saline. At 6 and 18 h after intratracheal instillation, we performed histological examination and bronchoalveolar lavage and assessed the lung wet/dry weight ratio as an index of acute lung injury. Then we measured the numbers of total cells and neutrophils and the levels of tumor necrosis factor (TNF)-α and cytokine-induced neutrophil chemoattractant (CINC) in bronchoalveolar lavage fluid (BALF). In addition, we evaluated BALF total protein and albumin levels as indexes of lung permeability. LPS instillation caused severe acute lung injury, as indicated by the histological findings and the lung wet/dry weight ratio. However, AM infusion attenuated these LPS-induced abnormalities. AM decreased the numbers of total cells and neutrophils and the levels of TNF-α and CINC in BALF. AM also reduced BALF total protein and albumin levels. In addition, AM significantly suppressed apoptosis of alveolar wall cells as indicated by cleaved caspase-3 staining. In conclusion, continuous infusion of AM ameliorated LPS-induced acute lung injury in rats. This beneficial effect of AM on acute lung injury may be mediated by inhibition of inflammation, hyperpermeability, and alveolar wall cell apoptosis.

apoptosis; hyperpermeability; inflammation

ACUTE RESPIRATORY DISTRESS syndrome (ARDS) is a life-threatening disease characterized by diffuse lung injury that leads to respiratory failure and death (2, 12). Its mortality remains high despite recent advances in intensive care (4, 38). Therefore, a novel therapeutic strategy for ARDS is desirable. Potential mechanisms that induce ARDS include lung inflammation and hyperpermeability (4, 36). Lung inflammation induces the production of various molecules that mediate lung injury such as arachidonic acid metabolites (2, 16), proteases (59), and free radicals (10, 40). Lung hyperpermeability contributes to the development of pulmonary edema, resulting in abnormal gas exchange. Furthermore, apoptosis of several cell types, including neutrophils, alveolar epithelial cells, and endothelial cells, is involved in the pathogenesis of acute lung injury in ARDS (9, 24, 26). Thus a therapeutic strategy against these abnormalities may be effective for the treatment of ARDS.

Adrenomedullin (AM) is an endogenous peptide that was originally isolated from human pheochromocytoma (20). It has been shown to have a variety of protective effects on the cardiovascular system in addition to vasodilator activity (6, 18, 27–29, 32). It has been shown to inhibit inflammatory cytokine production (13, 14, 53). AM also has been reported to reduce endothelial hyperpermeability through a cyclic adenosine 3′,5′-monophosphate-dependent mechanism (11). Furthermore, AM has been reported to protect against apoptosis through a phosphatidylinositol 3-kinase/Akt-dependent pathway (15, 19, 34, 39, 45). Considering that AM has been shown to attenuate organ injury in sepsis models (7, 41, 51), it may have protective effects against inflammation, hyperpermeability, and cell apoptosis, which are responsible for acute lung injury in ARDS. However, the effects and mechanisms of AM in acute lung injury remain unknown.

Lipopolysaccharide (LPS), a bacterial cell wall component, is a stimulus for the initiation of local acute inflammation. Intratracheal instillation of LPS in animals has gained wide acceptance as an experimental model of ARDS (5). Thus the purposes of this study were *1*) to investigate whether AM infusion ameliorates acute lung injury and *2*) to examine the underlying mechanisms responsible for the effects of AM on acute lung injury.

METHODS

Animals. All protocols were performed in accordance with the guidelines of the Animal Care Ethics Committee of the National Cardiovascular Center Research Institute. Adult male Sprague-Dawley rats weighing 180–200 g were used in this study. Rats were assigned to receive a continuous infusion of AM or vehicle and underwent intratracheal instillation of either LPS or 0.9% saline. This protocol resulted in the creation of four groups: sham rats given vehicle (Sham-Vehicle group; $n = 34$), sham rats treated with AM (Sham-AM group; $n = 34$), LPS rats given vehicle (LPS-Vehicle group; $n = 34$), and LPS rats treated with AM (LPS-AM group; $n = 34$).

Experimental protocol. After the rats were anesthetized by intraperitoneal injection of pentobarbital (30 mg/kg), they were given a

Address for reprint requests and other correspondence: N. Nagaya, Dept. of Regenerative Medicine and Tissue Engineering, National Cardiovascular Center Research Institute, 5-7-1 Fujishirodai, Suita, Osaka 565-8565, Japan (e-mail: nnagaya@ri.ncvc.go.jp).

The costs of publication of this article were defrayed in part by the payment of page charges. The article must therefore be hereby marked "*advertisement*" in accordance with 18 U.S.C. Section 1734 solely to indicate this fact.

continuous intravenous infusion of either AM or saline vehicle via a microosmotic pump (2001D; Alzet, Palo Alto, CA). Briefly, an osmotic pump was filled with either AM or saline and was set to deliver a dose of 0.1 $\mu g \cdot kg^{-1} \cdot min^{-1}$, attached to a catheter (PE-60) placed in the left jugular vein, and implanted subcutaneously between the scapulae. The rats were allowed to recover from the anesthesia and were maintained on standard rat chow. Two hours after implantation, the rats were intratracheally injected with either 1 mg/kg LPS (*Escherichia coli* 055:B5; Sigma, St. Louis, MO) dissolved in 0.3 ml saline or vehicle (0.3 ml saline) under anesthesia. We measured the LPS content in the saline by using the Limulus amoebocyte lysate test (E-Toxate; Sigma). The saline used in this study contained <6 pg LPS/ml. After recovery from anesthesia, the animals were again maintained on standard rat chow. The animals showed no sign of distress with this procedure. All rats remained alive after intratracheal instillation of LPS.

The animals were killed with an overdose of pentobarbital, and the following parameters were analyzed. Bronchoalveolar lavage (BAL) was performed at 6 and 18 h after intratracheal instillation (n = 8 each). Histological examination was performed in another group of rats at 6 and 18 h (n = 5 each). To estimate the circulating level of AM, blood sampling was performed at 18 h. To evaluate the severity of acute lung injury, the lung wet/dry weight ratio was calculated at 18 h in the rats that were not subjected to BAL or histological examination (n = 8 each). The wet lung weight was measured immediately after dissection, and the dried lung weight was estimated after oven drying at 60°C for 72 h. The experimental design is summarized in Fig. 1.

Preparation of AM. Recombinant human AM was obtained from Shionogi (Osaka, Japan). The homogeneity of AM was confirmed by reverse-phase high-performance liquid chromatography and amino acid analysis. AM was stored at −80°C until the time of preparation for infusion.

Measurement of AM. Blood was immediately transferred into a chilled glass tube containing disodium EDTA (1 mg/ml) and aprotinin (500 U/ml) and was centrifuged immediately at 4°C. Plasma samples were frozen and stored at −80°C. Human AM was measured by using a specific immunoradiometric assay kit (AM RIA; Shionogi) (33). Rat AM was also measured by using this assay kit with some modifications, as reported previously (31).

BAL analysis. BAL was performed through a tracheal cannula with 5 ml saline solution. This procedure was performed twice. A 500-μl aliquot of BAL fluid (BALF) was reserved for determination of the total number of cells and cell differentiation, and the remainder was centrifuged immediately at 700 *g* for 5 min at 4°C. The supernatant of BALF was immediately stored at −80°C before assays. The total number of cells was counted by using a standard hemocytometer. Cell differentiation was examined by counting at least 200 cells on a smear prepared by using cytospin and Wright-Giemsa staining.

Tumor necrosis factor-α and cytokine-induced neutrophil chemoattractant assays. BALF tumor necrosis factor (TNF)-α and cytokine-induced neutrophil chemoattractant (CINC) levels were measured by using a rat TNF-α ELISA kit (BioSource International, Camarillo, CA) and a rat Gro/CINC-1 kit (Amersham Biosciences, Piscataway, NJ), respectively.

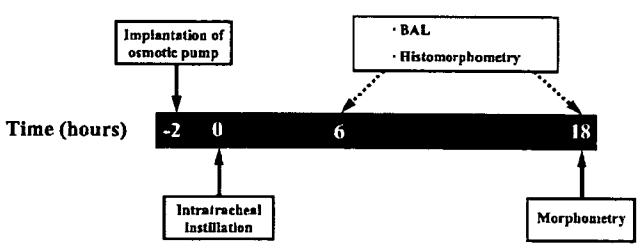

Fig. 1. Study protocol timeline. Implantation of osmotic pump, intratracheal instillation, bronchoalveolar lavage (BAL), histomorphometry, and morphometry were performed.

Total protein and albumin assays. To investigate the effect of AM on lung permeability, BALF total protein and albumin levels were measured by using a Bradford assay (Bio-Rad, Tokyo, Japan) and a bromcresol green assay (Sigma), respectively.

Histological examination. The lungs were fixed with 4% paraformaldehyde and were embedded in paraffin. Paraffin sections 4-μm thick were stained with hematoxylin and eosin for examination by light microscopy. Lung injury was graded from 0 (normal) to 4 (severe) in four categories: interstitial inflammation, neutrophil infiltration, congestion, and edema (42). Lung-injury score was calculated by adding the individual scores for each category. Grading was performed by a blinded pathologist. Lung-injury score for each animal was calculated as the mean of four lung sections. Paraffin sections were obtained from individual rats at 6 or 18 h after intratracheal instillation (n = 5 per group).

Immunohistochemical study. To investigate the effect of AM on lung apoptosis, tissue sections were stained for cleaved caspase-3, a key executor of apoptosis, by using a rabbit polyclonal anti-cleaved caspase-3 antibody (Cell Signaling Technology, Beverly, MA). The number of cleaved caspase-3-positive alveolar wall cells was determined in 10 randomly chosen fields (×400) per section. The percentage of cleaved caspase-3-positive inflammatory cells was calculated (number of cleaved caspase-3-positive inflammatory cells/total number of inflammatory cells × 100) in 10 randomly chosen fields (×400) per section, as previously described (21). The mean of four sections per animal was determined in a blinded manner. Paraffin sections 4-μm thick were obtained from the lungs at 6 h after intratracheal instillation (n = 5 per group).

Statistical analysis. All data are expressed as means ± SE. All data have been tested for normality by using the Shapiro-Wilk normality test and were determined to have a normal distribution. Homogeneity of variance was tested by using Bartlett's test. When Bartlett's test indicated that the group comparisons had equal variance, one-way ANOVA and Newman-Keuls' test were used. When the group data showed unequal variance, nonparametric statistical analysis was used. A value of $P < 0.05$ was considered statistically significant.

RESULTS

Inhibition of LPS-induced acute lung injury by AM. Photomicrographs showed that intratracheal instillation of LPS caused infiltration of inflammatory cells into the lung interstitium and alveolar spaces, alveolar wall thickening, and intra-alveolar exudation at 6 and 18 h after LPS instillation. (Fig. 2*A*). However, AM infusion attenuated these histological changes. Semiquantitative assessment using lung-injury score demonstrated that the degree of lung injury in the LPS-AM group was lower than that in the LPS-Vehicle group at 6 and 18 h after LPS instillation (Fig. 2*B*). The lung wet/dry weight ratio was significantly increased at 18 h after LPS instillation (Fig. 3). AM infusion significantly attenuated the increase in the lung wet/dry weight ratio compared with vehicle. AM infusion did not induce any changes in lung histology and the lung wet/dry weight ratio in Sham rats. AM infusion tended to decrease systemic blood pressure but did not cause severe hypotension in LPS rats (121 ± 8 to 114 ± 10 mmHg).

Plasma AM level. Plasma AM level was significantly higher in LPS rats than in Sham rats (10 ± 1 vs. 3 ± 1 fmol/ml, $P <$ 0.05). Furthermore, the level was markedly increased in LPS

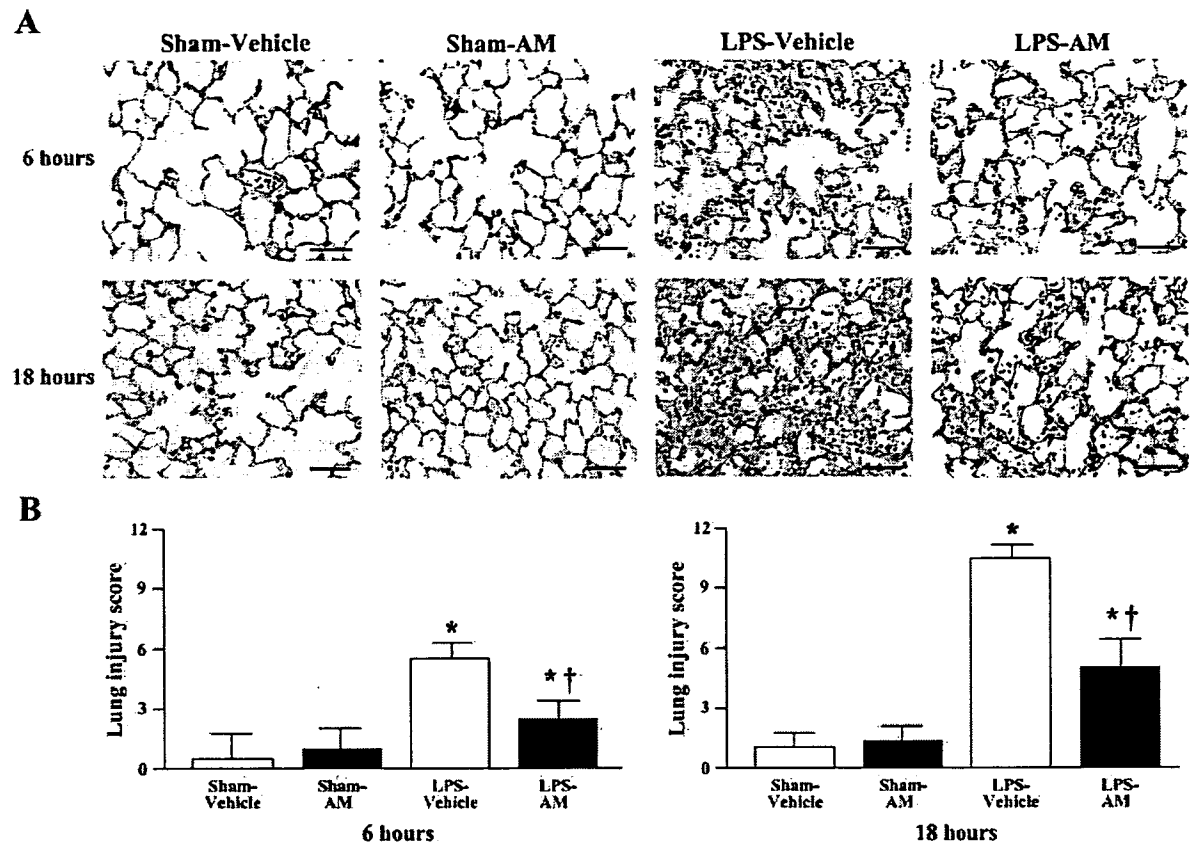

Fig. 2. *A*: representative photomicrographs of lung tissues stained with hematoxylin and eosin at 6 and 18 h after lipopolysaccharide (LPS) instillation. Intratracheal instillation of LPS caused infiltration of inflammatory cells into lung interstitium and alveolar spaces, alveolar wall thickening, and intra-alveolar exudation. Scale bars, 50 μm. *B*: semiquantitative analysis of lung tissues by lung-injury score. Lung-injury score was significantly decreased in LPS-adrenomedullin (AM) group compared with LPS-Vehicle (saline) group. Data are means ± SE. *$P < 0.05$ vs. Sham-Vehicle; †$P < 0.05$ vs. LPS-Vehicle.

rats treated with AM (32 ± 3 fmol/ml) compared with in those given vehicle ($P < 0.01$). These results suggest that the administered AM reached pharmacological levels.

Effects of AM on LPS-induced lung inflammation. The recovery rate of BALF was >80% in all groups. The numbers of total cells and neutrophils were significantly increased at 6 and 18 h after LPS instillation (Fig. 4, *A* and *B*). However, the numbers of these cells in the LPS-AM group were significantly lower than those in the LPS-Vehicle group. The BALF TNF-α level was significantly increased at 6 and 18 h after LPS instillation (Fig. 4*C*). Similarly, the BALF CINC level was significantly increased after LPS instillation (Fig. 4*D*). AM infusion significantly attenuated the increases in BALF TNF-α and CINC levels. AM infusion did not significantly alter BAL data in sham rats.

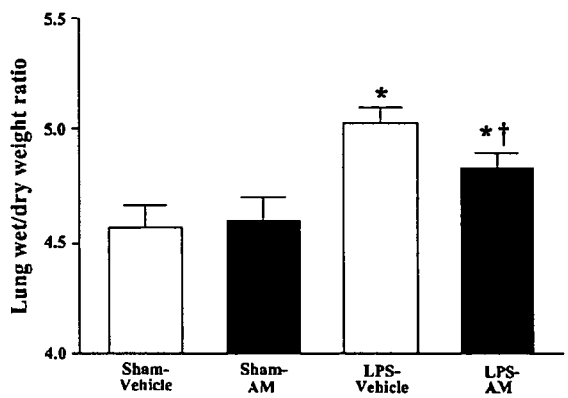

Fig. 3. Effect of AM infusion on lung weight after LPS instillation. Data are means ± SE. *$P < 0.05$ vs. Sham-Vehicle; †$P < 0.05$ vs. LPS-Vehicle.

Effects of AM on LPS-induced lung hyperpermeability. The BALF total protein and albumin levels, markers for lung permeability, were significantly increased at 6 and 18 h after LPS instillation (Fig. 5). AM infusion significantly attenuated the increases in BALF total protein and albumin levels.

Effect of AM on LPS-induced alveolar wall cell apoptosis. Cleaved caspase-3-positive cells were frequently observed in the alveolar wall at 6 h after LPS instillation (Fig. 6*A*). AM infusion markedly decreased cleaved caspase-3-positive cells in the alveolar wall. Semiquantitative analysis demonstrated a significant increase in the number of cleaved caspase-3-positive alveolar wall cells after LPS instillation, and the increase in the LPS-AM group was significantly attenuated compared with that in the LPS-Vehicle group (Fig. 6*B*). AM infusion did not significantly change the percentage of cleaved caspase-3-positive inflammatory cells compared with vehicle infusion (3 ± 2 vs. 4 ± 1%).

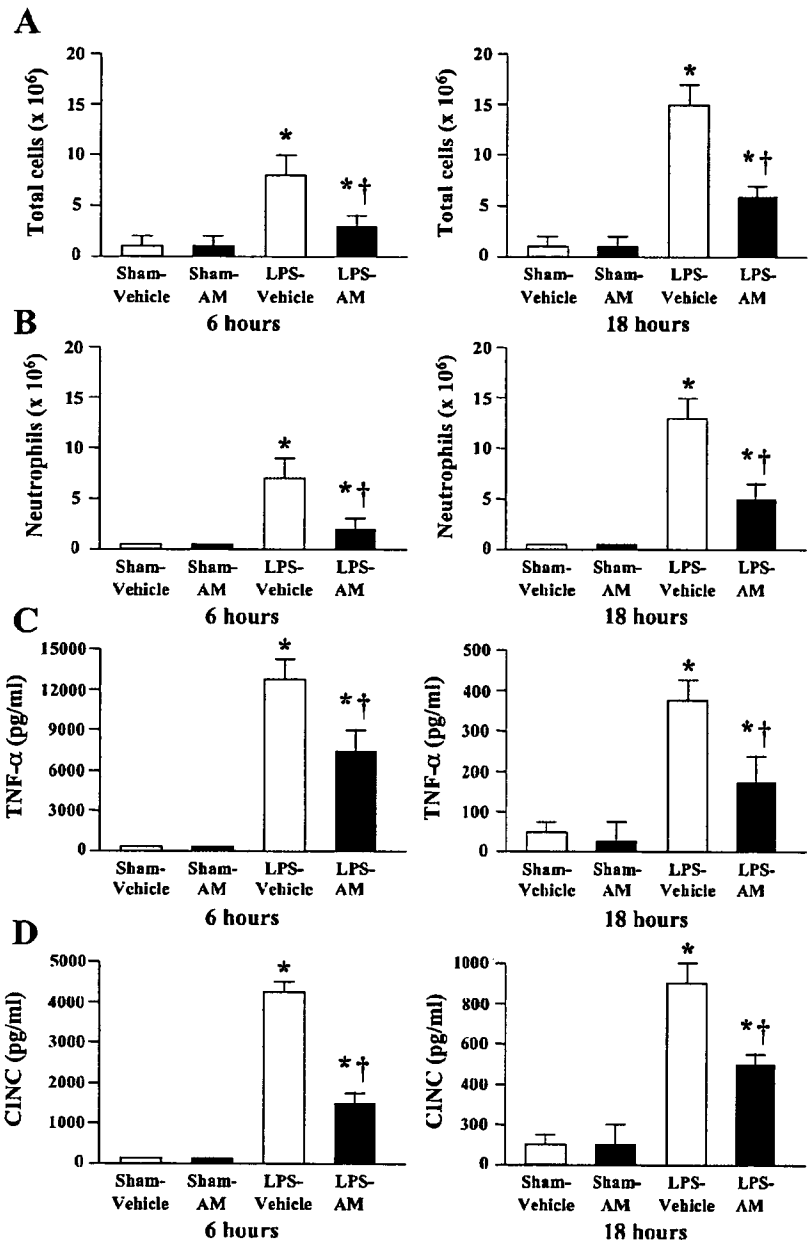

Fig. 4. Effects of AM infusion on numbers of total cells (*A*) and neutrophils (*B*) and levels of tumor necrosis factor (TNF)-α (C) and cytokine-induced neutrophil chemoattractant (CINC; D) in BAL fluid (BALF) at 6 and 18 h after LPS instillation. Numbers of total cells and neutrophils were significantly increased at 6 and 18 h after LPS instillation. However, numbers of these cells in LPS-AM group were significantly lower than those in LPS-Vehicle group. AM infusion significantly decreased BALF TNF-α and CINC levels. Data are means ± SE. $*P < 0.05$ vs. Sham-Vehicle; $\dagger P < 0.05$ vs. LPS-Vehicle.

DISCUSSION

In the present study, we demonstrated that AM infusion *1*) ameliorated LPS-induced histological changes and attenuated the increase in lung weight after LPS instillation, *2*) decreased the numbers of total cells and neutrophils and the levels of TNF-α and CINC in BALF, *3*) reduced the levels of total protein and albumin in BALF, and *4*) inhibited apoptosis of alveolar wall cells.

In the present study, intratracheal instillation of LPS was used to produce a model of ARDS in rats. Acute lung injury was histologically confirmed in rats subjected to LPS instillation. LPS instillation also increased the lung wet/dry weight ratio, an index of acute lung injury. AM infusion significantly attenuated these abnormalities, suggesting that AM ameliorates LPS-induced acute lung injury in rats. We also demonstrated that the circulating level of AM was significantly increased after intratracheal instillation of LPS, which is consistent with previous observations that AM expression is increased in animals and humans with acute lung injury (1, 46). In the present study, AM infusion caused a significant additional increase in the circulating level of AM in rats subjected to LPS instillation. Thus supplementation of AM may produce beneficial actions at pharmacological levels. However, the underlying mechanisms still remain unclear. Considering the variety of protective effects of AM, the present study investigated the effects of AM on lung inflammation, permeability, and cell apoptosis, all of which are responsible for acute lung injury.

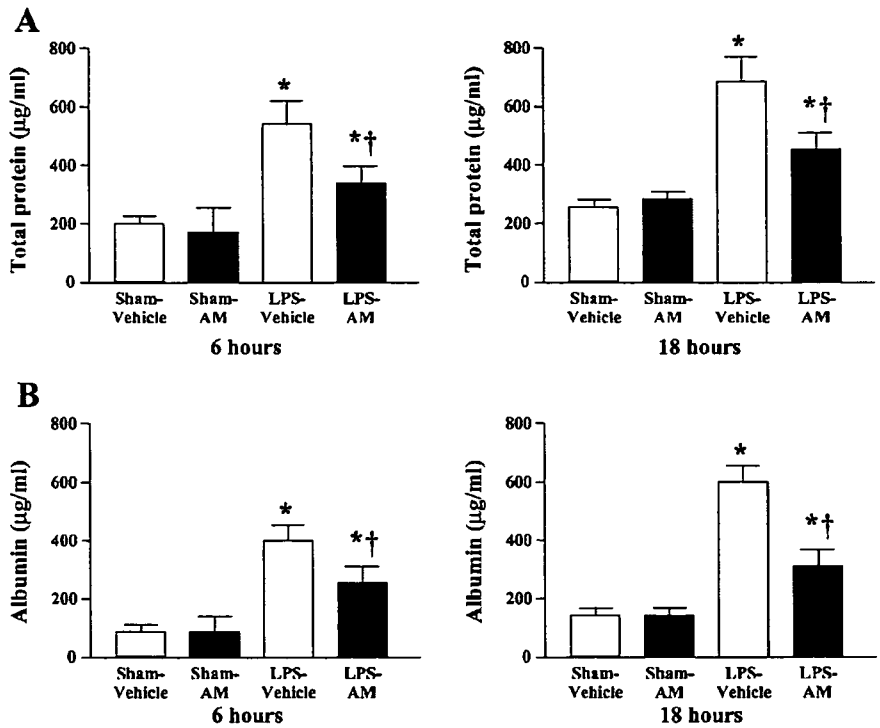

Fig. 5. Effects of adrenomedullin (AM) infusion on BALF total protein (*A*) and albumin (*B*) at 6 and 18 h after LPS instillation. AM infusion significantly reduced BALF total protein and albumin levels. Data are means ± SE. *$P < 0.05$ vs. Sham-Vehicle; †$P < 0.05$ vs. LPS-Vehicle.

LPS is known to induce severe lung inflammation through the migration and activation of inflammatory cells. In particular, neutrophils are considered to be responsible (54). The present study also showed that LPS instillation markedly increased the number of neutrophils in BALF. However, AM infusion significantly attenuated the increase in neutrophils. These findings suggest that AM infusion ameliorates LPS-induced lung inflammation at least in part through inhibition of neutrophil infiltration. Several investigations have identified that several cytokines play pivotal roles in the initiation and development of inflammation (44, 47, 57). LPS has been reported to induce the production of several cytokines in vivo

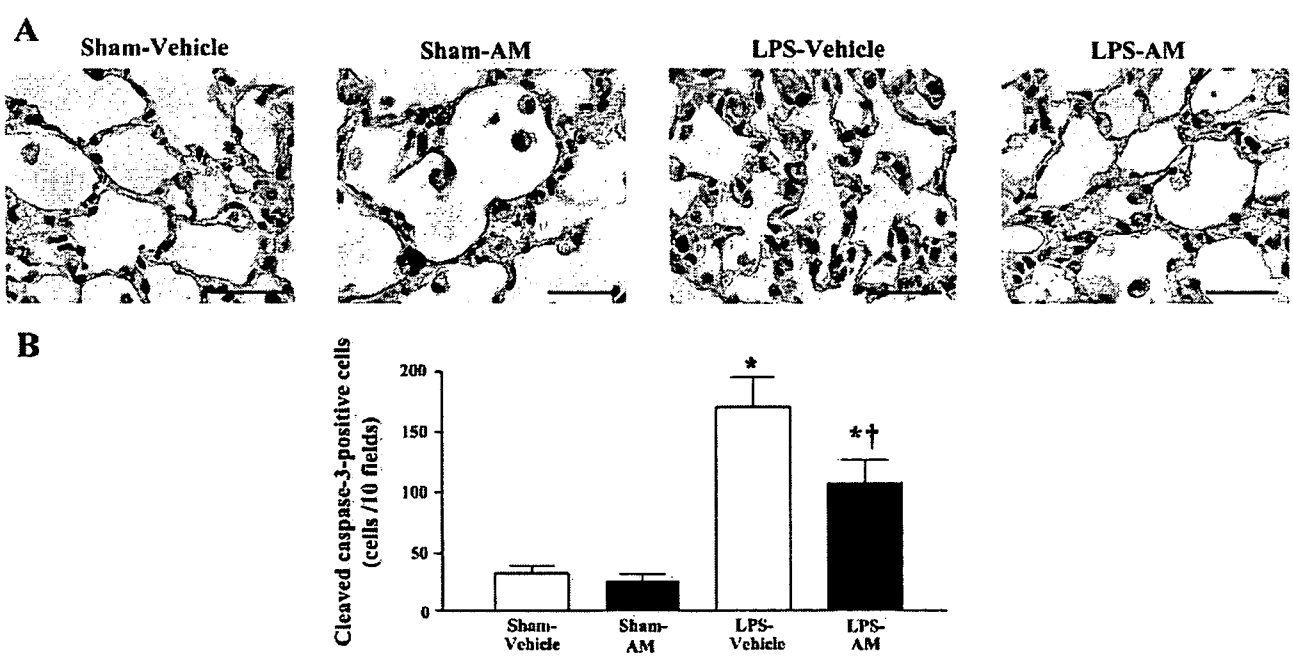

Fig. 6. *A*: immunohistochemical demonstration of cleaved caspase-3 antigen, a marker for cell apoptosis, in lungs at 6 h after LPS instillation. Scale bars, 20 μm. *B*: semiquantitative analysis of cleaved caspase-3-positive alveolar wall cells. Number of cleaved caspase-3-positive alveolar wall cells was significantly decreased in LPS-AM group compared with LPS-Vehicle group. Data are means ± SE. *$P < 0.05$ vs. Sham-Vehicle; †$P < 0.05$ vs. LPS-Vehicle.

and in vitro (3, 8). In fact, in the present study, BALF TNF-α and CINC levels were markedly increased in rats with LPS instillation. TNF-α, a proinflammatory cytokine, participates in several important processes involved in the inflammatory response (23, 48–50, 55). On the other hand, CINC, a member of the CXC chemokine family, plays a pivotal role in neutrophil migration in rats (47, 56). These findings suggest that these cytokines are potentially important mediators of LPS-induced lung inflammation. It should be noted that AM infusion significantly decreased BALF TNF-α and CINC levels. Our results may be supported by earlier in vitro findings that AM reduces LPS-stimulated secretion of TNF-α and CINC from macrophages (17, 58). These findings suggest that AM infusion suppresses LPS-induced lung inflammation through inhibition of cytokine production.

Lung hyperpermeability is also involved in the pathogenesis of ARDS (4, 36). Intratracheal instillation of LPS has been shown to injure pulmonary endothelial and epithelial cell layers and to increase lung permeability, resulting in pulmonary edema (25). Recent studies have shown that a reduction of lung hyperpermeability protects against LPS-induced acute lung injury (35, 43). In the present study, LPS instillation significantly increased BALF total protein and albumin levels, markers for lung permeability. AM infusion attenuated the LPS-induced increases in BALF total protein and albumin levels. Recently, AM has been shown to reduce endothelial hyperpermeability through a cyclic adenosine 3′,5′-monophosphate-dependent mechanism in perfused rabbit lungs (11). Thus the therapeutic effects of AM on acute lung injury may be mediated by a reduction of lung hyperpermeability.

Apoptosis of several cell types, including neutrophils, alveolar epithelial cells, and endothelial cells, is involved in the pathogenesis of acute lung injury in ARDS (9, 24, 26). In fact, in the present study, LPS instillation significantly increased the number of apoptotic alveolar wall cells. AM infusion attenuated the LPS-induced increase in the number of apoptotic alveolar wall cells, although it did not affect inflammatory cell apoptosis. Cell apoptosis and survival in the alveolar wall play an important role in the maintenance of lung homeostasis. Several studies have shown that apoptosis inhibitors attenuate LPS-induced acute lung injury in animals (21, 52). Inhibition of alveolar wall cell apoptosis has been shown to be associated with the attenuation of LPS-induced acute lung injury (21, 30). In addition, AM has been shown to protect against apoptosis in vivo and in vitro (15, 19, 34, 39, 45). These findings suggest that AM infusion ameliorates LPS-induced acute lung injury at least in part through inhibition of alveolar wall cell apoptosis. Further studies are necessary to clarify whether the hemodynamic effect of AM influences LPS-induced acute lung injury.

In conclusion, continuous infusion of AM ameliorated LPS-induced acute lung injury in rats. This beneficial effect of AM may be mediated by inhibition of inflammation, hyperpermeability, and alveolar wall cell apoptosis.

GRANTS

This work was supported by a Research Grant for Cardiovascular Disease (16C-6) from the Ministry of Health, Labour and Welfare, by the Program for Promotion of Fundamental Studies in Health Sciences of the National Institute of Biomedical Innovation (NIBIO), and by a Grant-in-Aid for Exploratory Research from the Ministry of Education, Culture, Sports, Science, and Technology.

REFERENCES

1. **Agorreta J, Zulueta JJ, Montuenga LM, Garayoa M.** Adrenomedullin expression in a rat model of acute lung injury induced by hypoxia and LPS. *Am J Physiol Lung Cell Mol Physiol* 288: L536–L545, 2005.
2. **Artigas A, Bernard GR, Carlet J, Dreyfuss D, Gattinoni L, Hudson L, Lamy M, Marini JJ, Matthay MA, Pinsky MR.** The American-European Consensus Conference on ARDS, part 2: ventilatory, pharmacologic, supportive therapy, study design strategies, and issues related to recovery and remodeling. Acute respiratory distress syndrome. *Am J Respir Crit Care Med* 157: 1332–1347, 1998.
3. **Bannerman DD, Goldblum SE.** Mechanisms of bacterial lipopolysaccharide-induced endothelial apoptosis. *Am J Physiol Lung Cell Mol Physiol* 284: L899–L914, 2003.
4. **Bernard GR, Artigas A, Brigham KL, Carlet J, Falke K, Hudson L, Lamy M, Legall JR, Morris A, Spragg R.** The American-European Consensus Conference on ARDS. Definitions, mechanisms, relevant outcomes, and clinical trial coordination. *Am J Respir Crit Care Med* 149: 818–824, 1994.
5. **Brigham KL, Meyrick B.** Endotoxin and lung injury. *Am Rev Respir Dis* 133: 913–927, 1986.
6. **Eto T, Kato J, Kitamura K.** Regulation of production and secretion of adrenomedullin in the cardiovascular system. *Regul Pept* 112: 61–69, 2003.
7. **Fowler DE, Yang S, Zhou M, Chaudry IH, Simms HH, Wang P.** Adrenomedullin and adrenomedullin binding protein-1: their role in the septic response. *J Surg Res* 109: 175–181, 2003.
8. **Glauser MP, Zanetti G, Baumgartner JD, Cohen J.** Septic shock: pathogenesis. *Lancet* 338: 732–736, 1991.
9. **Hashimoto S, Kobayashi A, Kooguchi K, Kitamura Y, Onodera H, Nakajima H.** Upregulation of two death pathways of perforin/granzyme and FasL/Fas in septic acute respiratory distress syndrome. *Am J Respir Crit Care Med* 161: 237–243, 2000.
10. **Hassoun PM, Yu FS, Cote CG, Zulueta JJ, Sawhney R, Skinner KA, Skinner HB, Parks DA, Lanzillo JJ.** Upregulation of xanthine oxidase by lipopolysaccharide, interleukin-1, and hypoxia. Role in acute lung injury. *Am J Respir Crit Care Med* 158: 299–305, 1998.
11. **Hippenstiel S, Witzenrath M, Schmeck B, Hocke A, Krisp M, Krull M, Seybold J, Seeger W, Rascher W, Schutte H.** Adrenomedullin reduces endothelial hyperpermeability. *Circ Res* 91: 618–625, 2002.
12. **Hudson LD, Milberg JA, Anardi D, Maunder RJ.** Clinical risks for development of the acute respiratory distress syndrome. *Am J Respir Crit Care Med* 151: 293–301, 1995.
13. **Isumi Y, Kubo A, Katafuchi T, Kangawa K, Minamino N.** Adrenomedullin suppresses interleukin-1beta-induced tumor necrosis factor-alpha production in Swiss 3T3 cells. *FEBS Lett* 463: 110–114, 1999.
14. **Iwamoto M, Osajima A, Tamura M, Suda T, Ota T, Kanegae K, Watanabe Y, Kabashima N, Anai H, Nakashima Y.** Adrenomedullin inhibits pressure-induced mesangial MCP-1 expression through activation of protein kinase A. *J Nephrol* 16: 673–681, 2003.
15. **Iwase T, Nagaya N, Fujii T, Itoh T, Ishibashi-Ueda H, Yamagishi M, Miyatake K, Matsumoto T, Kitamura S, Kangawa K.** Adrenomedullin enhances angiogenic potency of bone marrow transplantation in a rat model of hindlimb ischemia. *Circulation* 111: 356–362, 2005.
16. **Jourdan KB, Evans TW, Goldstraw P, Mitchell JA.** Isoprostanes and PGE2 production in human isolated pulmonary artery smooth muscle cells: concomitant and differential release. *FASEB J* 13: 1025–1030, 1999.
17. **Kamoi H, Kanazawa H, Hirata K, Kurihara N, Yano Y, Otani S.** Adrenomedullin inhibits the secretion of cytokine-induced neutrophil chemoattractant, a member of the interleukin-8 family, from rat alveolar macrophages. *Biochem Biophys Res Commun* 211: 1031–1035, 1995.
18. **Kato J, Tsuruda T, Kitamura K, Eto T.** Adrenomedullin: a possible autocrine or paracrine hormone in the cardiac ventricles. *Hypertens Res* 26: S113–S119, 2003.
19. **Kato H, Shichiri M, Marumo F, Hirata Y.** Adrenomedullin as an autocrine/paracrine apoptosis survival factor for rat endothelial cells. *Endocrinology* 138: 2615–2620, 1997.
20. **Kitamura K, Kangawa K, Kawamoto M, Ichiki Y, Nakamura S, Matsuo H, Eto T.** Adrenomedullin: a novel hypotensive peptide isolated from human pheochromocytoma. *Biochem Biophys Res Commun* 192: 553–560, 1993.
21. **Kitamura Y, Hashimoto S, Mizuta N, Kobayashi A, Kooguchi K, Fujiwara I, Nakajima H.** Fas/FasL-dependent apoptosis of alveolar cells

after lipopolysaccharide-induced lung injury in mice. *Am J Respir Crit Care Med* 163: 762–769, 2001.
22. **Kubo K, Amari T, Kaneki T, Hanaoka M, Hayano T, Miyahara T, Koyama S, Koizumi T, Fujimoto K, Kobayashi T.** A 21-aminosteroid, U-74006F, attenuates endotoxin-induced lung injury in awake sheep. *Respirology* 4: 167–172, 1994.
23. **Kuwano K, Hara N.** Signal transduction pathways of apoptosis and inflammation induced by the tumor necrosis factor receptor family. *Am J Respir Cell Mol Biol* 22: 147–149, 2000.
24. **Li X, Shu R, Filippatos G, Uhal BD.** Apoptosis in lung injury and remodeling. *J Appl Physiol* 97: 1535–1542, 2004.
25. **Li XY, Donaldson K, MacNee W.** Lipopolysaccharide-induced alveolar epithelial permeability: the role of nitric oxide. *Am J Respir Crit Care Med* 157: 1027–1033, 1998.
26. **Matute-Bello G, Martin TR.** Science review: apoptosis in acute lung injury. *Crit Care* 7: 355–358, 2003.
27. **Nagaya N, Kyotani S, Uematsu M, Ueno K, Oya H, Nakanishi N, Shirai M, Mori H, Miyatake K, Kangawa K.** Effects of adrenomedullin inhalation on hemodynamics and exercise capacity in patients with idiopathic pulmonary arterial hypertension. *Circulation* 109: 351–356, 2004.
28. **Nagaya N, Mori H, Murakami S, Kangawa K, Kitamura S.** Adrenomedullin: angiogenesis and gene therapy. *Am J Physiol Regul Integr Comp Physiol* 288: R1432–R1437, 2005.
29. **Nagaya N, Satoh T, Nishikimi T, Uematsu M, Furuichi S, Sakamaki F, Oya H, Kyotani S, Nakanishi N, Goto Y, Masuda Y, Miyatake K, Kangawa K.** Hemodynamic, renal, and hormonal effects of adrenomedullin infusion in patients with congestive heart failure. *Circulation* 101: 498–503, 2000.
30. **Nakagomi T, Kitada O, Kuribayashi K, Yoshikawa H, Ozawa K, Ogawa S, Matsuyama T.** The 150-kilodalton oxygen-regulated protein ameliorates lipopolysaccharide-induced acute lung injury in mice. *Am J Pathol* 165: 1279–1288, 2004.
31. **Nishikimi T, Mori Y, Kobayashi N, Tadokoro K, Wang X, Akimoto K, Yoshihara F, Kangawa K, Matsuoka H.** Renoprotective effect of chronic adrenomedullin infusion in Dahl salt-sensitive rats. *Hypertension* 39: 1077–1082, 2002.
32. **Nishikimi T, Yoshihara F, Mori Y, Kangawa K, Matsuoka H.** Cardioprotective effect of adrenomedullin in heart failure. *Hypertens Res* 26: S121–S127, 2003.
33. **Ohta H, Tsuji T, Asai S, Tanizaki S, Sasakura K, Teraoka H, Kitamura K, Kangawa K.** A simple immunoradiometric assay for measuring the entire molecule of adrenomedullin in human plasma. *Clin Chim Acta* 287: 131–143, 1999.
34. **Okumura H, Nagaya N, Itoh T, Okano I, Hino J, Mori K, Tsukamoto Y, Ishibashi-Ueda H, Miwa S, Tambara K.** Adrenomedullin infusion attenuates myocardial ischemia/reperfusion injury through the phosphatidylinositol 3-kinase/Akt-dependent pathway. *Circulation* 109: 242–248, 2004.
35. **Peng X, Hassoun PM, Sammani S, McVerry BJ, Burne MJ, Rabb H, Pearse D, Tuder RM, Garcia JG.** Protective effects of sphingosine 1-phosphate in murine endotoxin-induced inflammatory lung injury. *Am J Respir Crit Care Med* 169: 1245–1251, 2004.
36. **Pittet JF, Mackersie RC, Martin TR, Matthay MA.** Biological markers of acute lung injury: prognostic and pathogenetic significance. *Am J Respir Crit Care Med* 155: 1187–1205, 1997.
37. **Riedemann NC, Guo RF, Ward PA.** The enigma of sepsis. *J Clin Invest* 112: 460–467, 2003.
38. **Rubenfeld GD, Caldwell E, Peabody E, Weaver J, Martin DP, Neff M, Stern EJ, Hudson LD.** Incidence and outcomes of acute lung injury. *N Engl J Med* 353: 1685–1693, 2005.
39. **Sata M, Kakoki M, Nagata D, Nishimatsu H, Suzuki E, Aoyagi T, Sugiura S, Kojima H, Nagano T, Kangawa K.** Adrenomedullin and nitric oxide inhibit human endothelial cell apoptosis via a cyclic GMP-independent mechanism. *Hypertension* 36: 83–88, 2000.
40. **Sato K, Suga M, Akaike T, Fujii S, Muranaka H, Doi T, Maeda H, Ando M.** Therapeutic effect of erythromycin on influenza virus-induced lung injury in mice. *Am J Respir Crit Care Med* 157: 853–857, 1998.
41. **Shindo T, Kurihara H, Maemura K, Kurihara Y, Kuwaki T, Izumida T, Minamino N, Ju KH, Morita H, Oh-hashi Y.** Hypotension and resistance to lipopolysaccharide-induced shock in transgenic mice overexpressing adrenomedullin in their vasculature. *Circulation* 101: 2309–2316, 2000.
42. **Simons RK, Maier RV, Chi EY.** Pulmonary effects of continuous endotoxin infusion in the rat. *Circ Shock* 33: 233–243, 1991.
43. **Speyer CL, Neff TA, Warner RL, Guo RF, Sarma JV, Riedemann NC, Murphy ME, Murphy HS, Ward PA.** Regulatory effects of iNOS on acute lung inflammatory responses in mice. *Am J Pathol* 163: 2319–2328, 2003.
44. **Strieter RM, Kunkel SL, Keane MP, Standiford TJ.** Chemokines in lung injury: Thomas A. Neff Lecture. *Chest* 116: 103S–110S, 1999.
45. **Tokunaga N, Nagaya N, Shirai M, Tanaka E, Ishibashi-Ueda H, Harada-Shiba M, Kanda M, Ito T, Shimizu W, Tabata Y, Uematsu M, Nishigami K, Sano S, Kangawa K, Mori H.** Adrenomedullin gene transfer induces therapeutic angiogenesis in a rabbit model of chronic hind limb ischemia: benefits of a novel nonviral vector, gelatin. *Circulation* 109: 526–531, 2004.
46. **Ueda S, Nishio K, Minamino N, Kubo A, Akai Y, Kangawa K, Matsuo H, Fujimura Y, Yoshioka A, Masui K, Doi N, Murao Y, Miyamoto S.** Increased plasma levels of adrenomedullin in patients with systemic inflammatory response syndrome. *Am J Respir Crit Care Med* 160: 132–136, 1999.
47. **Ulich TR, Howard SC, Remick DG, Wittwer A, Yi ES, Yin S, Guo K, Welply JK, Williams JH.** Intratracheal administration of endotoxin and cytokines. VI. Antiserum to CINC inhibits acute inflammation. *Am J Physiol Lung Cell Mol Physiol* 268: L245–L250, 1995.
48. **Ulich TR, Watson LR, Yin SM, Guo KZ, Wang P, Thang H, del Castillo J.** The intratracheal administration of endotoxin and cytokines. I. Characterization of LPS-induced IL-1 and TNF mRNA expression and the LPS-, IL-1-, and TNF-induced inflammatory infiltrate. *Am J Pathol* 138: 1485–1496, 1991.
49. **Ulich TR, Yi ES, Yin S, Smith C, Remick D.** Intratracheal administration of endotoxin and cytokines. VII. The soluble interleukin-1 receptor and the soluble tumor necrosis factor receptor II (p80) inhibit acute inflammation. *Clin Immunol Immunopathol* 72: 137–140, 1994.
50. **Ulich TR, Yin SM, Guo KZ, del Castillo J, Eisenberg SP, Thompson RC.** The intratracheal administration of endotoxin and cytokines. III. The interleukin-1 (IL-1) receptor antagonist inhibits endotoxin- and IL-1-induced acute inflammation. *Am J Pathol* 138: 521–524, 1991.
51. **Yang S, Zhou M, Fowler DE, Wang P.** Mechanisms of the beneficial effect of adrenomedullin and adrenomedullin-binding protein-1 in sepsis: down-regulation of proinflammatory cytokines. *Crit Care Med* 30: 2729–2735, 2002.
52. **Vernooy JH, Dentener MA, van Suylen RJ, Buurman WA, Wouters EF.** Intratracheal instillation of lipopolysaccharide in mice induces apoptosis in bronchial epithelial cells: no role for tumor necrosis factor-alpha and infiltrating neutrophils. *Am J Respir Cell Mol Biol* 24: 569–576, 2001.
53. **von der Hardt K, Kandler MA, Popp K, Schoof E, Chada M, Rascher W, Dotsch J.** Aerosolized adrenomedullin suppresses pulmonary transforming growth factor-beta1 and interleukin-1 beta gene expression in vivo. *Eur J Pharmacol* 457: 71–76, 2002.
54. **Wagner JG, Roth RA.** Neutrophil migration during endotoxemia. *J Leukoc Biol* 66: 10–24, 1999.
55. **Ward PA.** Role of complement, chemokines, and regulatory cytokines in acute lung injury. *Ann NY Acad Sci* 796: 104–112, 1996.
56. **Watanabe K, Koizumi F, Kurashige Y, Tsurufuji S, Nakagawa H.** Rat CINC, a member of the interleukin-8 family, is a neutrophil-specific chemoattractant in vivo. *Exp Mol Pathol* 55: 30–37, 1991.
57. **Wiedermann FJ, Mayr AJ, Kaneider NC, Fuchs D, Mutz NJ, Schobersberger W.** Alveolar granulocyte colony-stimulating factor and alpha-chemokines in relation to serum levels, pulmonary neutrophilia, and severity of lung injury in ARDS. *Chest* 125: 212–219, 2004.
58. **Wu R, Zhou M, Wang P.** Adrenomedullin and adrenomedullin binding protein-1 downregulate TNF-alpha in macrophage cell line and rat Kupffer cells. *Regul Pept* 112: 19–26, 2003.
59. **Yasui S, Nagai A, Aoshiba K, Ozawa Y, Kakuta Y, Konno K.** A specific neutrophil elastase inhibitor (ONO-5046.Na) attenuates LPS-induced acute lung inflammation in the hamster. *Eur Respir J* 8: 1293–1299, 1995.

Nephrol Dial Transplant (2007) 22: 2263–2268
doi:10.1093/ndt/gfm029
Advance Access publication 29 March 2007

Original Article

NDT
Nephrology Dialysis Transplantation

Midregional proadrenomedullin reflects cardiac dysfunction in haemodialysis patients with cardiovascular disease

Fumiki Yoshihara[1], Andrea Ernst[2], Nils G. Morgenthaler[3], Takeshi Horio[1], Satoko Nakamura[1], Hajime Nakahama[1], Hiroto Nakata[1], Andreas Bergmann[2,3], Kenji Kangawa[4] and Yuhei Kawano[1]

[1]Division of Hypertension and Nephrology, National Cardiovascular Center, Suita, Osaka, Japan, [2]SphingoTec GmbH, Tulpenweg 6, D-16556 Borgsdorf, [3]Research Department, B.R.A.H.M.S AG, Neuendorfstrasse 25, D-16761 Hennigsdorf, Germany and [4]Research Institute, National Cardiovascular Center, Suita, Osaka, Japan

Abstract

Background. Although adrenomedullin is an indicator of cardiac dysfunction in haemodialysis patients, the clinical significance of midregional proadrenomedullin has not been elucidated.

Objectives. We evaluated whether midregional proadrenomedullin reflects cardiac dysfunction, systemic inflammation or blood volume in haemodialysis patients.

Methods. Plasma midregional proadrenomedullin, C-reactive protein and delta body weight (indicating excessive blood volume), and two-dimensional as well as Doppler echocardiographic variables were measured just before haemodialysis in 70 patients with cardiovascular disease.

Results. The median value of midregional proadrenomedullin was 1.93 nmol/l before haemodialysis, and these levels were significantly reduced following haemodialysis. Log [midregional proadrenomedullin] was positively correlated with left ventricular end-systolic volume index, diameter of inferior vena cava, C-reactive protein and delta body weight ($r=0.328$, $r=0.421$, $r=0.356$, $r=0.364$), and negatively with blood pressure, deceleration time of an early diastolic filling wave, pulmonary venous flow velocity ratio and left ventricular ejection fraction ($r=-0.330$, $r=-0.324$, $r=-0.479$, $r=-0.373$). Multivariate regression analysis revealed that pulmonary venous flow velocity ratio, diameter of inferior vena cava and C-reactive protein were independently related factors for midregional proadrenomedullin concentration.

Conclusion. Plasma midregional proadrenomedullin levels increase in association with cardiac dysfunction, systemic inflammatory status and systemic blood volume in haemodialysis patients with concomitant cardiovascular disease.

Correspondence and offprint requests to: Fumiki Yoshihara, MD, 5-7-1 Fujishirodai, Suita, Osaka 565-8565, Japan.
Email: fyoshi@ri.ncvc.go.jp

Keywords: cardiac dysfunction; excessive blood volume; haemodialysis; midregional proadrenomedullin; systemic inflammatory status

Introduction

Cardiovascular disease [1], excessive blood volume [2] and systemic inflammation [3] are the major causes of mortality in haemodialysis patients. Early diagnosis and treatment of these processes in haemodialysis patients may lead to improved survival. For this purpose, a non-invasive biochemical testing method would be ideal for screening and monitoring cardiac status, blood volume and inflammatory state.

Plasma adrenomedullin levels are elevated in left ventricular (LV) failure [4], myocardial infarction [5] and peripheral arterial occlusive disease [6], and these levels increase according to disease severity. Plasma adrenomedullin levels are additionally increased in haemodialysis patients [7] and these increases may be involved in the regulation of systemic blood pressure [7], and may reflect changes in systemic blood volume [8] in these patients. We also recently reported that adrenomedullin reflects cardiac dysfunction, excessive blood volume and inflammation, thereby proving to be a good predictor of mortality and cardiovascular morbidity in haemodialysis patients with cardiovascular disease [9].

Because adrenomedullin has a short half-life (22 min) in human plasma and is regulated by a proteolytic enzyme [10], the pre-analytical conditions of the plasma samples, particularly the storage temperature, may influence the final test results. Furthermore, several other factors may influence adrenomedullin measurement, including a binding protein that may be present in human plasma, which may have a specific inhibitory effect on the adrenomedullin radioimmunoassay [11]. Also, autocrine or paracrine interactions between adrenomedullin and

its receptors in the vicinity of release may lead to a removal of adrenomedullin from the circulation. Taken together, these pre-analytical factors may lead to an underestimation of the true adrenomedullin values by immunoassays.

Adrenomedullin is derived from a larger precursor peptide (prepro-adrenomedullin; 185 amino acids) by posttranslational processing [12]. During the processing of prepro-adrenomedullin, two peptides flank Adrenomedullin: one midregional part of proadrenomedullin (proadrenomedullin 45–92) and the COOH terminus of the molecule (proadrenomedullin 153–185). We have recently reported the technical characterization of this midregional proadrenomedullin (MR-proADM) sandwich immunoassay [13]. In contrast to mature adrenomedullin, MR-proADM is stable in plasma at room temperature for at least 72 h. MR-proADM probably has no physiological effects and its apparent stability may be attributable to this lack of function because only bioactive substances require careful regulation by proteolysis. The released amounts of MR-proADM may directly reflect levels of adrenomedullin. In addition, circulating MR-proADM is unlikely to be influenced by a binding protein, making it suitable for immunometric analysis. Although we recently reported that MR-proADM is increased in patients with cardiovascular disease [13], a more detailed analysis of the relationship between plasma MR-proADM concentration and cardiac function or cardiovascular disease severity is still lacking.

Therefore, we conducted the present study to investigate whether plasma MR-proADM accurately reflects cardiac dysfunction, removal of fluid volume by ultrafiltration, and systemic inflammatory status in haemodialysis patients admitted for evaluation of cardiovascular disease. We also performed pilot work to assess whether MR-proADM levels are predictive of subsequent mortality.

Methods

Patients

Seventy consecutive haemodialysis patients (51 men, 19 women; mean age, 65 ± 10 years), admitted to the National Cardiovascular Center for evaluation of cardiovascular disease, were enrolled in the present study. Patients having atrial fibrillation, overt pulmonary effusion, or pulmonary congestion were excluded from the present study. All patients underwent regular haemodialysis for 3–4 h three times weekly (Monday, Wednesday and Friday). Written informed consent was obtained from all patients. The procedures were in accordance with the Helsinki Declaration of 1975 (and as revised in 1983). After release from our institute, patients were followed up for an average 14.7 months. All-cause deaths were recorded.

Echocardiographic measurement

A skilled echocardiographer without knowledge of the clinical features of the patients performed the echocardiographic studies using a cardiac ultrasound unit (Sonos 5500; Philips Medical Systems, Andover, MA) just prior to haemodialysis treatment, as previously reported [9]. Left ventricular end-diastolic volume index (LVEDVI), left ventricular end-systolic volume index (LVESVI) and left ventricular ejection fraction (LVEF) were calculated using the modified Simpson method according to the recommendations of the American Society of Echocardiography [14].

To assess left ventricular (LV) diastolic function, LV diastolic filling (LV inflow) was examined using Doppler echocardiography. The LV diastolic filling pattern was obtained with the sample volume at the tips of the mitral valve in the apical four-chamber view and was recorded at the end-expiratory phase during quiet breathing. Peak velocity of early diastolic filling (E) and peak velocity of atrial filling (A) were recorded, and the E/A ratio was calculated. The deceleration time (DcT) was measured as the time between the top of the E wave and the point at which the descending part of the E wave or its asymptote crossed the zero line.

After LV inflow velocities were examined, pulmonary venous flow velocities were obtained from the apical four-chamber view and recorded at end-expiration. The pulsed Doppler sample volume was set at 0.5–1.0 cm into the upper right pulmonary vein. Peak forward flow velocities during ventricular systole (S) and diastole (D) were measured, and the S/D ratio was calculated. Echocardiographic parameters were obtained in 51 patients. LV inflow velocities and pulmonary venous flow velocities were obtained in 50 patients, because in the other patients it proved technically difficult to evaluate these variables.

Blood pressure, excessive blood volume, blood sampling and assay for MR-proADM

Blood pressure was measured with a mercury sphygmomanometer in the supine position after supine rest of 5 min or longer before blood sampling. Excessive blood volume before haemodialysis was defined as the fluid volume removal by ultrafiltration during haemodialysis (=delta body weight). Blood was withdrawn through the shunt before and after haemodialysis to measure MR-proADM, and was transferred into a chilled glass tube containing disodium EDTA and aprotinin. The blood was centrifuged immediately at 4°C, and plasma was frozen and stored at −80°C until assay. Plasma levels of MR-proADM were measured using a specific immunoassay system as previously reported [13]. The personnel responsible for measuring MR-proADM were blinded to the clinical and ultrasound status of the patients. Plasma C-reactive protein (CRP) levels were also measured, but only before haemodialysis by using the standardized methods in an autoanalyser.

Blood sampling and the echocardiographic studies were performed just before haemodialysis because of the need to evaluate the relationship between humoral factors and cardiac function in concurrence with excessive blood volume.

Statistical analysis

Data are expressed as means ± SD or using the median and interquartile range. Statistical comparisons were made with the Wilcoxon rank-tests or Mann–Whitney U-tests between two groups. Significant differences between more than two

groups were evaluated by Kruskal–Wallis tests with subsequent Scheffe's multiple comparison tests. Because MR-proADM data were not normally distributed, log [MR-proADM] was used in the correlations and regression models. Univariate linear and multivariate stepwise regression analyses were used to detect factors related to two-dimensional, Doppler echocardiographic parameters, plasma CRP concentrations or removal fluid volume to log [MR-proADM]. Event-free curves were estimated by the Kaplan–Meier product-limited method and compared with the Mantel (log-rank) test. The prognostic value of MR-proADM was tested by Cox's proportional-hazards regression analysis. Differences were considered to be statistically significant when the P value was <0.05.

Results

Clinical characteristics of the study population and echocardiographic findings just before haemodialysis are listed in Tables 1 and 2, respectively. All patients had a normal cardiac sinus rhythm, but each had cardiovascular disease as shown in Table 1.

The median values and interquartile ranges of MR-proADM before and after haemodialysis in patients with cardiovascular disease are shown in Figure 1. Haemodialysis significantly decreased plasma concentrations of MR-proADM.

In univariate linear regression analysis, log [MR-proADM] was significantly and negatively correlated with systolic blood pressure (SBP), DcT, S/D ratio and LVEF, and positively with LVESVI©, CRP and delta body weight (BW) (Table 3). Multivariate regression analysis revealed that S/D ratio, "diameter of inferior vena cava (IVC)" and CRP were independently related factors for MR-ProAM (Table 3). Log [MR-proADM] tended to be positively correlated with the E/A ratio and LVEDVI, but these did not reach statistical significance.

To evaluate the possible effects of LV diastolic dysfunction on plasma concentrations of MR-proADM, we compared levels among patients with $E/A > 1$ and $E/A \leq 1$, patients with DcT < 180 ms and DcT ≥ 180 ms, and patients with S/D < 1, $1 \leq$ S/D < 2 and S/D ≥ 2. In patients with DcT < 180 ms, plasma MR-proAM concentrations were significantly higher than those with DcT ≥ 180 ms. Furthermore, in patients with $S/D < 1$, plasma MR-proADM concentrations were significantly greater than in patients with $S/D \geq 2$ (Figure 2).

Nine patents died during the 14.7-month follow-up period. Event-free Kaplan–Meier curves comparing MR-proADM cut-off values are shown in Figure 3. We used the median value of MR-proADM (=1.93 nmol/l) as the cut-off in the present study. Seven of 34 patients with MR-proADM levels >1.93 nmol/l died and 2 of 36 with levels of 1.93 nmol/l or lower died during the follow-up period. Patients with greater MR-proADM levels had a greater death rate than those with lower MR-proADM levels (log-rank test, $P = 0.0346$).

Table 1. Clinical characteristics of the study population

Age (years)	64.5 ± 10.3
Sex (Male/female)	51/19
Duration of haemodialysis (years)	6.5 ± 7.9
Cause of renal failure (number of patients)	
Chronic glomerulonephritis	26
Diabetic nephropathy	21
Nephrosclerosis	9
Polycystic kidney disease	4
Renal stone	2
Renal tuberculosis	1
Cardiovascular disease (number of events)	
Coronary artery disease	42
Peripheral arterial occlusive disease	22
Hypertensive heart disease	10
Cerebrovascular attack	9
Aortic aneurysm	6
Aortic valve stenosis	4
Ventricular tachycardia	3
Paroxysmal supraventricular tachycardia	1
Primary pulmonary hypertension	1
Cardiac tumour	1
Heart rate (bpm)	71 ± 12
Systolic blood pressure (mmHg)	145 ± 22
Diastolic blood pressure (mmHg)	70 ± 11
Plasma albumin level (g/dl)	3.6 ± 0.4
Plasma MR-proADM level (nmol/l)	1.93 (1.42, 2.40)
Delta body weight (kg)	1.88 ± 1.12
Plasma C-reactive protein level (mg/dl)	1.13 ± 1.81

Data are expressed as numbers or means ± SD or medians (interquartile range).

Table 2. Echocardiographic findings just before haemodialysis

DcT (msec)	248.7 ± 58.7
E/A ratio	0.90 ± 0.28
S/D ratio	1.49 ± 0.47
LVEDVI (ml/m^2)	59.1 ± 21.7
LVESVI (ml/m^2)	26.2 ± 18.1
LVEF (%)	59.3 ± 13.8
IVC (mm)	16.4 ± 4.0

Data are expressed as means ± SD. Abbreviations: A, peak velocity of atrial filling; E, peak velocity of early diastolic filling; DcT, deceleration time of early diastolic filling; S, peak forward-flow velocity during ventricular systole; D, peak forward-flow velocity during ventricular diastole; LVEDVI, left ventricular end-diastolic volume index; LVESVI, left ventricular end-systolic volume index; LVEF, left ventricular ejection fraction; IVC, diameter of inferior vena cava.

Discussion

In the present study, we showed that (i) the median concentration of MR-proADM was 1.93 nmol/l in a cohort of haemodialysis patients with cardiovascular disease; (ii) plasma MR-proADM concentrations were negatively correlated with blood pressure, DcT, S/D and LVEF, and positively correlated with LVESVI and IVC in these same patients, suggesting that plasma MR-proADM reflects LV diastolic and systolic dysfunction, which were defined as decreases in DcT, S/D and LVEF and increases in LVESVI; (iii) plasma

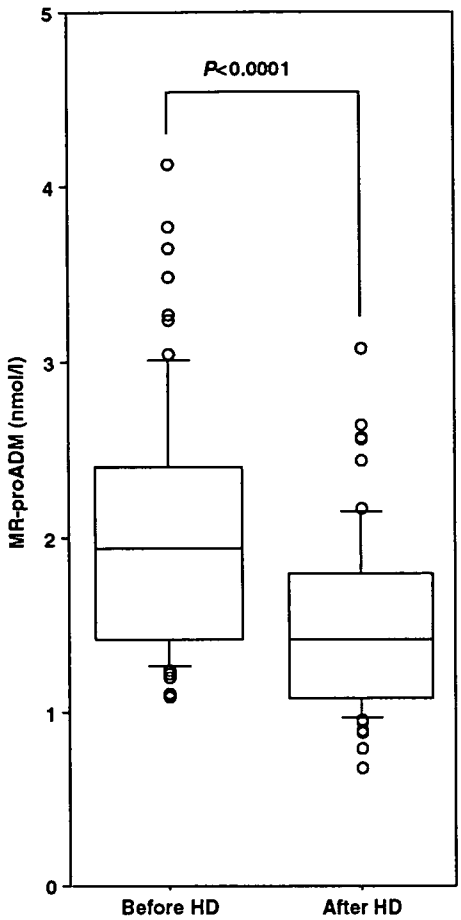

Fig. 1. Plasma midregional proadrenomedullin (MR-proADM) levels before and after haemodialysis (HD) in patients with cardiovascular disease.

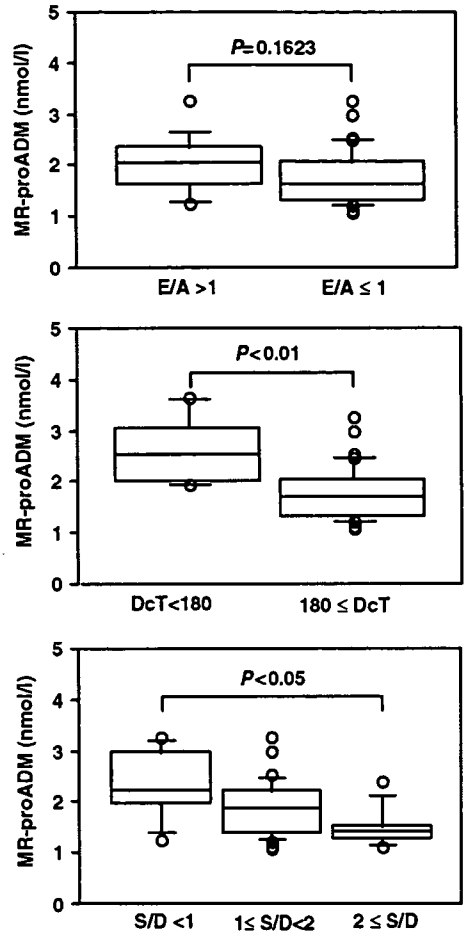

Fig. 2. Midregional proadrenomedullin (MR-proADM) levels in the DcT < 180 ($N=6$) and DcT ≥ 180 groups ($N=44$), in the $E/A > 1$ ($N=12$) and $E/A \leq 1$ groups ($N=38$), and in the $S/D < 1$ ($N=7$), $1 \leq S/D < 2$ ($N=35$) and $S/D \geq 2$ ($N=8$) groups.

Table 3. Univariate correlation between log (MR-proADM) and age, echocardiographic findings, C-reactive protein levels and delta body weight in haemodialysis patients

	Univariate		Mutivariate	
	R	*P*	Beta-coefficient	*P*
SBP (mmHg)	−0.330	0.0053	NS	
DcT (msec)	−0.324	0.0189	NS	
S/D ratio	−0.479	0.0004	−0.266	0.0368
LVESVI (ml/m^2)	0.328	0.0200	NS	
LVEF (%)	−0.373	0.0077	NS	
IVC (mm)	0.421	0.0015	0.300	0.0153
CRP (mg/dl)	0.356	0.0025	0.410	0.0009
Delta BW (kg)	0.364	0.0020	NS	

For Abbreviations, see Table 2. SBP, systolic blood pressure, CRP, C-reactive protein; BW, body weight.

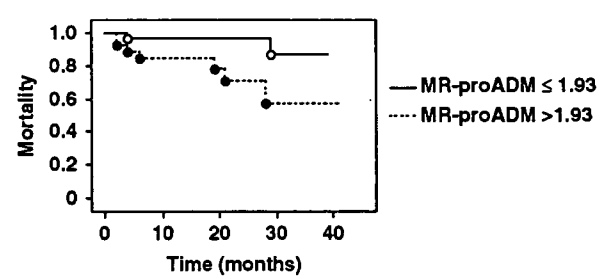

Fig. 3. Kaplan–Meier event-free curves in haemodialysis patients classified according to plasma midregional proadrenomedullin (MR-proADM) level [≤1.93 nmol/l ($N=36$; mortality number: 2) or >1.93 nmol/l ($N=34$; mortality number: 7)] (log-rank test, $P=0.0346$).

MR-proADM increased in association with systemic inflammatory status and/or removal fluid volume during haemodialysis ultrafiltration; (iv) patients with high MR-proADM had a higher mortality rate than those with low MR-proADM during the 14.7-month follow-up period.

We recently reported a MR-proADM mean value of 0.33 nmol/l in healthy individuals [13]. This was subsequently confirmed in other cohorts of healthy

individuals (N.G.M. unpublished data). We did not evaluate MR-proADM concentrations in healthy controls in the present study. Nevertheless, compared with these previous reports, the high median MR-proADM concentration of 1.93 nmol/l in our patients is more than 5-fold higher than in healthy subjects, suggesting that MR-proADM is clearly increased in patients with end-stage renal disease. Because the kidney is the most important clearance organ for circulating peptides such as BNP [15], the correlation coefficient between plasma BNP level and cardiac catheterization data was weakened, despite increased plasma BNP levels in patients with renal dysfunction compared to those with preserved renal function in the intensive care unit. Thus, renal failure resulting in a decrease in peptide clearance may be one possible reason for the increase in plasma MR-proADM concentrations in these patients. In addition, renal failure is well known to cause body fluid retention resulting in volume overload. Volume overload in turn increases shear stress in the arteries of the extremities [16]. Previous reports demonstrated that volume overload by itself increased cardiac biventricular adrenomedullin production [17], and that shear stress also increased adrenomedullin production in vascular endothelial cells [18]. We found a positive correlation between MR-proADM concentration and excessive blood volume in our patients, suggesting that the increased production of adrenomedullin in cardiac ventricles and the vascular endothelium resulted in increased plasma MR-proADM levels in patients with end-stage renal disease.

Plasma MR-proADM concentrations were negatively correlated with systemic blood pressure in our patients. In other studies with haemodialysis patients, plasma adrenomedullin levels have also been reported to be increased and negatively correlated with systemic blood pressure [7]. Given that adrenomedullin has a potent vasodilatory effect, the negative correlation between MR-proADM and systemic blood pressure in the present study suggests that adrenomedullin may be involved in lowering blood pressure in haemodialysis patients. Alternatively, the negative correlation between MR-proADM and systemic blood pressure may be secondary to reduced LV systolic function resulting in low blood pressure in association with an increase in plasma MR-proADM levels.

We previously reported that MR-proADM concentrations are increased in patients with cardiovascular disease [13]. However, there were no data to document the relationship between MR-proADM levels and cardiac function. Here, we report that plasma MR-proADM concentrations related to not only LV systolic dysfunction, which was defined as reduced LVEF, but also to diastolic dysfunction defined as reduced DcT, by the *S/D* ratio, and by an increased *E/A* ratio. This suggests that in the present study the plasma MR-proADM concentration may reflect reduced LV systolic and diastolic function. Numerous previous studies showed that plasma adrenomedullin levels were increased in LV failure [4], myocardial infarction [5] and peripheral arterial occlusive disease [6], and these levels increased according to disease severity. Thus, the concomitant cardiovascular disease in our haemodialysis patients may have led to cardiovascular dysfunction, resulting in increased cardiac adrenomedullin production and increased plasma MR-proADM level.

Increasing levels of CRP have been associated with increased risk of death in patients undergoing long-term haemodialysis [3]. In the present study, there was a positive correlation between plasma MR-proAM and plasma CRP concentrations. Previous reports demonstrated that tumour necrosis factor alpha, which is one of the most common inflammation-related cytokines, increased basal secretion of adrenomedullin in a cultured monocyte/macrophage cell line [19]. Furthermore, plasma levels of MR-proADM were markedly increased in patients with sepsis, and these increases may be helpful in individual risk assessment in septic patients [20], where MR-proADM showed an especially strong association with the APACHE II score. Thus, plasma MR-proADM concentrations may provide an indication of chronic inflammatory status in haemodialysis patients that is independent of other cardiac disease conditions.

Study limitations

Although the results of our survival analysis were limited to a small sample pilot population, elevated plasma MR-proADM concentrations predicted a poorer prognosis in our patients. Since cardiovascular disease [1], excessive blood volume [2] and systemic inflammation [3] are the major causes of mortality in haemodialysis patients, our findings that plasma MR-proADM reflected LV systolic and diastolic dysfunction and excessive blood volume are in concordance with these observations. If these findings are confirmed in a much larger sample study, plasma MR-proADM concentrations in haemodialysis patients may provide a tool for physicians to evaluate the severity of LV dysfunction, excessive blood volume and systemic inflammatory condition, and to manage these problems in haemodialysis patients with cardiovascular diseases. We performed echocardiographical studies to non-invasively evaluate LV diastolic and systolic function and remodelling. This was done instead of left-sided and right-sided catheterizations, which are more precise methods for these evaluations. The echocardiographical studies were performed just before dialysis. Because predialysis volume overload may affect both echocardiographical parameters and plasma levels of MR-proADM, individual differences in delta body weight may have altered the relationship between these parameters and MR-proADM in our patients. Concomitant cardiovascular disease was disproportionately distributed in the present study in that coronary artery disease was more frequent than the other cardiovascular diseases. Furthermore,